DEPARTMENT OF THE INTERIOR
U.S. GEOLOGICAL SURVEY

The Shape of the Earthquake Coda: Implications for Coda Magnitude Relations

Barry F. Hirshorn
and
Allan G. Lindh

U.S. Geological Survey
345 Middlefield Road -- MS977
Menlo Park, CA 94025

30 August 1995

OPEN-FILE REPORT 95-674

ABSTRACT

The relationship between coda magnitude and coda duration results from the particular shape of the coda decay envelope, $A_c(\omega,t)$, as a function of time [*Herrmann*, 1975]. If $A_c(\omega,t) = st^{-a}$ [*Aki*, 1969], then the duration magnitude is

$$M_D = k + a * \log_{10}(\tau)\,, \tag{1}$$

where k is a constant proportional to the sum of $\log_{10}(s)$ and the gain of the recording instrument and, τ, the coda duration, is the time measured from the origin time. If, however, $A_c(\omega,t) = st^{-a}\, e^{\frac{-b(\omega)}{\log_{10} e}t}$ [*Aki and Chouet*, 1975], then

$$M_D = k + a * \log_{10}(\tau) + b(\omega) * \tau\,, \tag{2}$$

[*Hirshorn, Lindh, and Allen*, 1988, 1989].

Using coda durations and multiple coda amplitude measurements from each seismogram, we derive a coda magnitude relationship for each of the two coda models of equations (1) and (2). The signals used to derive these relationships came from 13 vertical-component, short-period velocity seismometers, all operating at the same gain, recorded on the USGS Northern California Seismic Network (NCSN). These data came from 60 local earthquakes in the magnitude 3.2 to 5.7 range occurring in the central California coast ranges. Data from an additional set of 177 earthquakes occurring in the same regions as the derivation set, and 19 events over about M_L 5 occurring throughout Calfornia, were then used to test these relationships.

We use the coda amplitude data to estimate the slope of the coda decay envelope, $A_c(\omega,t)$, at various times after the direct S arrival, and solve for a and $b(\omega)$ in (2). The resulting values for a and $b(\omega)$ (1.51 and 0.0081) agree remarkably well with those obtained by *Aki and Chouet* [1975] (1.5 and 0.0232) in the frequency range of 1.5 to 16.0 Hz. The value of 1.51 for a also agrees with the theoretical expectation of *Frenkal and Wennerberg*'s [1987] energy flux model, and the geometrical spreading value that *Campillo et al.* [1984] found for P_g waves. Because a and $b(\omega)$ are functions of physical parameters, $a \sim$ (dimension of scattering volume) over 2, $b(\omega) \sim Q_c(\omega)^{-1}$, it should be possible to extend the formalism to other tectonic provinces with different scattering and absorption characteristics.

Our coda durations are determined by the time at which the average absolute value of the signal, measured on a two-second window, falls below a specific threshold. This very stable quantitative measure of signal duration, combined with coda magnitude relationships calibrated for larger events allows us to generate robust magnitude estimates. Coda estimates from the RTP and M_Z magnitude estimates are currently being determined for earthquakes of magnitude 3 and larger in real time, in northern and central California. Preliminary locations and magnitude estimates are usually available within about 5 minutes of the origin time of an earthquake. They form the backbone of the USGS's real-time earthquake hazard monitoring capability, and form an essential part of the foreshock monitoring effort underway as part of the Parkfield Prediction Experiment (*Bakun et al.*, [1987]).

INTRODUCTION

Following the work of *Richter* [1935] numerous magnitude scales have been introduced, most based on measurements of the amplitude of a specific seismic wave recorded by a specific type of band-limited seismograph. The amplitudes of the direct phases on which these scales have been based are strongly affected by the particular travel paths between source and reciever, and are sensitive to directional source radiation effects. Locally recorded coda durations, however, are nearly independent of epicentral distance or azimuth [*Bisztricsany*, 1958; *Soloviev*, 1965; *Tsumura*, 1967; *Lee et al.*, 1972; *Aki and Chouet*, 1975].

Because the shape of the coda decay envelope is the same within a given geographic region—independent of magnitude or the distance between source and reciever [*Aki*, 1969; *Aki and Chouet*, 1975; *Tsujiura*, 1978; *Aki*, 1980; *Rautian and Khalturin*, 1978; *Phillips and Aki*, 1986], coda duration can be a direct measure of source size [*Aki*, 1980]. For a given amplitude threshold for terminating the coda duration measurement, the larger the event, the longer the duration. This separation of source and path effects makes coda magnitude an attractive alternative to the classical approach of using direct body and surface wave amplitude measurements to determine magnitude [*Aki*, 1980].

The first attempt to use the duration of a seismic signal to estimate magnitude was made by *Bisctricsany* [1958], who found that the magnitude was linearly related to the duration of surface waves for earthquakes in the M 4 to 8 range. The duration method was later extended to local earthquakes by *Solov'ev* [1965], *Tsumura* [1967], *Lee et al.* [1972] and *Real and Teng* [1973]. They derived relationships between magnitude and total signal duration for different geographic regions. More recently *Eaton* [1992] has derived a duration magnitude scale using a large data set which spans an M_L range of about 0.5 to 6.0. His scale incorporates additional terms to correct for depths greater than 10 km, and for epicentral distances that fall outside of the 40 to 350 km range. All of these relationships have been parameterized as linear functions of *tau*:

$$M_D = k + a * \log_{10}(\tau) + c * \Delta\,, \tag{3}$$

where τ is the duration measured from the P-wave arrival time, and Δ is epicentral distance in kilometers. In the first part of this work we derive a coda magnitude relationship param-

eterized in this conventional way for estimating the size of magnitude 3 and larger events from τ measurements made on a suite of low-gain seismographs distributed throughout central California. The resulting formula,

$$M_Z = -0.71 + 2.95 \log_{10}(\tau) + 0.001 \Delta + \delta + \gamma , \quad (4)$$

where δ is a gain-normalized site correction, and γ is a correction for instrument gain, appears to provide a robust estimator of M_L for events as large as about M_L 6, and moment magintude 7.5

When plotting the local magnitude M_L versus the logarithm of duration, a slight curvature has been consistently observed. (*Lee et al.*, 1972, Figure 4—Figure (1) of this work; *Real and Teng*, 1973, Figures 5 and 6; *Lee and Wetmiller*, 1976, page 23; *Bakun and Lindh*, 1977, Figure 6b—Figure (2) of this work.) For example, studies of earthquakes in the M_L 1 to 3.5 range in central California have obtained smaller values for a, the slope of the $\log_{10}(\tau)$ term in equation (3), in the range of 1.0 to 2.2 (*Lee, Eaton, and Brabb*, [1971]; *Lee et al.* [1972]). In the work reported here we obtain a larger value for a for somewhat larger events, as have other workers in California and elsewhere (*Tsumura*, [1967]; *Crosson*, [1972]; *Real and Teng*, [1973]; *Herrmann*, [1975]; *Bakun and Lindh*, [1977]). (See Table 1 for a comparison of the value for a obtained by some of these studies.) It appears that the different values obtained are primarily a function of the magnitude range of the events considered—the larger the events, the steeper the slope. Clearly if one wishes to use a single formula to span events from magnitude 1 to 7 or larger, something other than the linear relation between M_L and log coda duration of equation (3) is required [*Bakun and Lindh*, 1977; *Michaelson and Bakun*, 1986].

In 1975, Herrmann demonstrated that if the amplitude of the coda envelope decays at a constant exponential rate $A_c(\omega, t) = s(\omega)t^{-a}$, where ω is the angular frequency, A_c is the amplitude of the coda amplitude as a function of time, and s is related to the source strength, then the coda magnitude can be described by equation (3). Here τ is defined as the time when the amplitude of the coda envelope decays to the cut-off criteria $\eta = A_c(\omega, \tau)$, specified for a system.

Aki and Chouet [1975] presented a body of theory and observation which showed that the coda envelope did not follow this simple power law decay, but required an additional

exponential term reflecting energy absorbtion, so that $A_c(\omega,t) = st^{-a}\ e^{\frac{-b(\omega)}{\log 10 * e}t}$. An extension of the logic of *Herrmann* [1975] to Aki and Chouet's coda model implies that the duration magnitude parameterization should be of the form:

$$M_D = k + a * \log_{10}(\tau) + b(\omega) * \tau \qquad (2)$$

[*Hirshorn, Lindh, and Allen*, 1988, 1989]. In the second part of this work we solve for a and $b(\omega)$ directly from the decay of coda amplitude. We then test the resulting magnitude relationships with τ and coda amplitude data from an independent test set.

DATA

Coda amplitude and duration data from a set of 256 earthquakes occurring in California between January 23, 1984 and April 4, 1993 were chosen for analysis; they have average local Richter magnitudes, M_L, ranging from 2.8 to 7.4 (Tables 2, 3, and 4, stars in Figures 3 and 4). We used local magnitude values calculated by the University of California Seismographic Stations [*Darragh et al.*, 1986; *McKenzie et al.*, 1987] from maximum trace amplitudes recorded on standard Wood–Anderson torsion seismographs. Because our objective was the estimation of magnitude for large events, we used only data from a subset of low-gain vertical seismometers from the Northern California Seismic Network (NCSN) (solid squares in Figures 3 and 4). These stations have the same frequency response and operating characteristics as the normal high-gain NCSN stations, but are operated at gains of 42–48 db instead of the 72–84 db gain at which the high-gain verticals are normally operated [*Eaton*, 1975, 1977].

A subset of 60 of these earthquakes, which we call the derivation set, were used to derive both magnitude relationships. These events occurred between September 24, 1985 and April 4, 1989—a period during which all of the low-gain instruments were operating at the same (48 db) gain. The source regions of these earthquakes span the central California coast ranges from Coalinga to the northern portion of the San Francisco bay area. They have average local Richter magnitudes, M_L, ranging from 3.2 to 5.7 (Table 2, stars in Figure 3).

Both relationships (equations 1 and 2 above) were then applied to the remaining 196 earthquakes, which we called the test set. One hundred and seventy seven of these test

events occurred in the same regions as the derivation set (Table 3, stars in Figure 4a). Nineteen others, including the Landers, Big Bear, Joshua Tree, and Petrolia mainshocks, were events over M_L 5 occurring elsewhere in California. (Table 4, stars in Figure 4b).

Coda Amplitudes

The coda amplitude data used in this study are generated in real time by *Allen*'s [1978] algorithm as implemented on multi-processor hardware designed and built by Jim Ellis and Sam Rodriguez. This Real Time Picker, or RTP, analyzes data from over 400 short-period seismometers telemetered on a continuous basis to a central recording site in Menlo Park, California.

In addition to the arrival time of the first P-wave, its polarity, and the average absolute value of the amplitudes of the first three peaks after the P-arrival, the RTP also reports a coda length and multiple coda amplitude measurements, A_n, for each seismogram. (Table 1 in *Hirshorn and Lindh* [1987] gives a more detailed description of the quantities reported by the RTP.)

Up to six A_n values are reported by the RTP for each seismogram—where A_n is the average absolute value of the amplitudes within a two-second window,

$$A_n = \frac{1}{200} \sum_{i=1}^{200} \mid A_i \mid \ . \tag{5}$$

The n reported windows correspond to the largest n consecutive values of t_k in Table 5 for which t_n is less than or equal to τ. (The sample times are listed in Table 5, and illustrated in Figure 5a.). These windows are chosen so they sample more or less evenly the unclipped portion of the coda.

Coda Durations

The coda duration data used in this study are generated by two independent data acquisition systems (the Caltech–USGS Seismic Processing (CUSP) system and the Real Time Processor (RTP) system), running in parallel on signals from over 400 short-period NCSN seismometers telemetered on a continuous basis to a central recording site in Menlo Park, California.

The coda duration, τ, is defined as the time measured from the onset of the first P-wave to that time when the average absolute value on a two-second window (A_n above) first falls below 60 millivolts. From the A_n and τ data, a weight is also derived which attempts to measure the quality of the coda length estimate. Thus, the algorithm produces a coda length, and a measure of its quality, for every station for which the RTP or CUSP systems are able to estimate a P-wave arrival time.

After large earthquakes, the coda amplitudes often stay above the 60 millivolt cutoff threshold for extended periods of time. In these cases it is impractical to wait for "normal" coda termination—*i.e.*, for A_n to decay to the coda cutoff amplitude. We derive a τ estimate before termination occurs by fitting a line to the A_n data in log–log (log (A_n) versus log (t_n)) space, and then extrapolating this line to the 60 millivolt threshold. This time is then taken as an estimate of τ (Figure 5b). Figure 6 is an example of a clipped record of the M_L 6.2 Halls Valley mainshock with a simple power law approximation of this form superimposed on an unclipped portion of the coda decay to illustrate this process. This curve is equivalent to the linear fit in log–log space. This method has provided very accurate magnitude estimates for a number of large California earthquakes—when "normal" coda termination was impossible. (Note, for example, the events over about magnitude six in Tables 3 and 4.) Table 6 is an example of the results using this method for the M_L 7.1 Loma Prieta mainshock of October 17, 1989.

The coda measurement scheme described here is inherently superior in many ways to traditional coda length determinations. Traditional coda length estimates have been based on peak-to-peak measurements falling below some threshold, either one centimeter on a standard viewing device [*Lee et al.*, 1972], or below the background noise level. By averaging over a two-second window the average-absolute-value algorithm described here severely smooths the seismogram and avoids most of the short-term fluctuations that bedevil peak-value amplitude measurements. By extrapolating the coda decay shape of events occurring closely in time, we obtain accurate coda magnitudes for large events occurring during energetic aftershock sequences. By providing quantitative measures of coda length at all possible stations, the algorithm removes the subjectivity of the traditional scheme. Finally, by providing a measure of the reliability of every coda length, we make it possible to obtain the best possible magnitude estimate from data sets of widely varying

quality.

PHYSICAL BASIS FOR THE CODA MAGNITUDE SCALE

Aki and Chouet [1975] described the amplitude of the coda envelope of local earthquakes, $A_c(\omega, t)$, by the general expression:

$$A_c(\omega, t) = \text{Source}\ (\omega)\ \text{Path}\ (\omega, t)\ \text{Site}\ (\omega) \tag{6}$$

for lapse times, t, measured from the earthquake origin time, greater than about twice the S-wave travel-time. The coda source factor, Source (ω) in (6), is a scale factor that embodies all of the information about the earthquake source [*Chouet et al.*, 1978]. The coda shape factor, Path (ω, t), descibes the amplitude of the coda envelope at lapse time t, for a unitary earthquake—it can be thought of as the impulse response of the earth and depends only on the wave propagation effects of the medium—including scattering and anelastic attenuation [*Aki*, 1980; *Ellsworth*, 1989]. Site (ω) is the effect on the coda amplitude due to the recieving site. This separation of source, path, and site effects, together with the assumption that the shape of the coda decay envelope, Path (ω, t), is constant in a given geographic region—independent of magnitude, and the distance between source and receiver [*Aki and Chouet*, 1975], forms the basis for the duration magnitude scale, M_D [*Aki*, 1980].

If M_D is proportional to $\log_{10}$ [Source (ω)] in (6) [*Aki*, 1980], and signal duration, τ, is defined as the time measured from the arrival of the first P-wave to that time when $A_c(\omega, t)$ decreases to some pre-set amplitude cutoff threshold, $\eta = A_c(\omega, \tau)$, then

$$M_D = \log_{10}\ \eta - \log_{10}\ [\text{Path}(\omega, \tau)] - \log_{10}\ [\text{Site}(\omega)] + K + \gamma \tag{7}$$

[*Herrmann*, 1975; *Aki*, 1980; *Ellsworth*, 1989], where K is an additive constant that sets the zero level of the magnitude scale, and γ is a correction for the gain of the recording station. (Specifically, $K = \log\left(\frac{A_{sys}}{A_0}\right)$, and $\gamma = \log\left(\frac{A_i}{A_{sys}}\right)$ where A_i is the gain of station i, A_{sys} is the gain of the system used to derive the scale, and A_0 the gain of the "zero level" earthquake.) For larger local earthquakes, when the signal duration, τ, is large compared to the travel time of the first P-arrival, we may substitute τ for duration measured from the origin time. Rearranging terms, (7) becomes:

$$M_D = k - \log_{10}\,[\mathrm{Path}(\omega,\tau)] - \delta + \gamma\,, \tag{8}$$

where $k = \log_{10}\,\eta + \log\left(\frac{A_{o\gamma s}}{A_o}\right)$, and $\delta = \log_{10}\,[\mathrm{Site}\,(\omega)]$; a correction for the site effect.

Thus, the shape of the coda decay envelope, Path (ω,t), in (8), completely determines the functional form of M_D's dependance on τ [*Herrmann*, 1975; *Aki*, 1980; *Hirshorn, Lindh and Allen*, 1988, 1989; *Ellsworth*, 1989]. We therefore consider the problem of finding the coda magnitude relationship to be one of finding the proper functional description for the coda shape factor.

Candidate Models for the Coda Shape Factor

We consider two models for the coda shape factor, Path (ω,t) in (8): *Model I*, the simple power law approximation [*Aki*, 1969],

$$\mathrm{Path}\,(t) = t^{-a}\,, \tag{9}$$

and *Model II*, the single back scattering model [*Aki and Chouet*, 1975],

$$\mathrm{Path}\,(\omega,t) = t^{-a}\,e^{\frac{-b(\omega)}{\log_{10} e}t}\,, \tag{10}$$

where $b(\omega) = (\log_{10} e)\frac{\omega}{2Q_c(\omega)}$. This model is equivalent to *Frankel and Wennerberg*'s [1987] energy flux model: $\mathrm{Path}\,(\omega,t) = t^{-1.5}\,e^{\frac{-b_i(\omega)}{\log_{10} e}t}\,\sqrt{1 - e^{\frac{-2b_s(\omega)}{\log_{10} e}t}}$, at times, as measured from the P arrival time of more than about 13 seconds.

Gain Corrections

Assuming a general expression for the coda magnitude of the form:

$$M_D = k - \log_{10}\,[\mathrm{Path}(\omega,\tau)] - \delta + \gamma\,, \tag{8}$$

the effect of a change in the log of the amplitude of the coda envelope , $\log_{10} A_c(\omega,t)$, on M_D can be written as:

$$\frac{\partial M_D}{\partial[\log_{10} A_c(\omega,t)]} = -\frac{\partial[\log_{10}\mathrm{Path}(\omega,\tau)]}{\partial[\log_{10} A_c(\omega,t)]}\,. \tag{11}$$

Since $\log_{10} A_c(\omega, t)$ and $\log_{10}$ Path (ω, t) are the same function of t by definition, $\Delta M_D = -\Delta \log_{10} A_c(\omega, t)$. The effect on M_D of a change in gain from A_1 to A_2 is then

$$-\log_{10} \frac{A_2}{A_1} . \tag{12}$$

ANALYSIS

We derived two duration magnitude relationships: M_Z and M_{Z2} from *Model I* and *Model II*, respectively, using coda duration (τ) and coda amplitude (A_n) data from the 60 earthquakes of the derivation set. Since all of the stations from which these signals came were operating at the same gain during this period, we were able to perform the derivations without considering the effect of station gain. We then tested M_Z and M_{Z2} with τ and A_n data from an additional set of 196 test events. During this time period, the gains were changing systematiclly (being lowered by 6db.) All of these events have at least two or more high confidence coda lengths. Only data with believable S-wave coda decays—as determined from a careful check of the reported A_n values, high signal-to-noise ratios, and high confidence P-arrival times—were used in the analysis. The events chosen all have epicentral location estimates accurate to within a few kilometers, but because of the small dependence of coda length on epicentral distance, even a large location error should have a negligible effect on duration magnitudes.

Model I

In the first part of this work we derive a coda magnitude relationship (M_Z) using the conventional parameterization of equation (8) for M_D:

$$M_Z = k + a * \log_{10}(\tau) + c\Delta + \delta + \gamma , \tag{13}$$

where Δ is epicentral distance in kilometers, δ is a correction for a given site's magnitude bias, and γ is a correction for station gain. Since the coda durations used to derive M_Z came from a suite of low-gain NCSN stations all operating at the same gain, we assumed that the gain correction, γ in (13), was equal to zero.

The procedure we have followed in obtaining our estimates of the coefficients in formula (13) is outlined below.

1. Preliminary estimates of k, a, and c in (13) were obtained from an examination of the relationship between M_L for each event, and the M_D estimate obtained by application of formula (3), to the low-gain codas. This resulted in an approximate formula for M_Z of

$$M_{Z_{ij}} = -0.495 + 2.67 \log_{10}(\tau_{ij}) + 0.001\,\Delta_{ij} + \delta_i\,, \tag{14}$$

for the ith measurement for the jth event.

2. Using this relation, an approximate average M_Z was computed for each event, these values were plotted against M_L for each event, and a least squares line fit to the data (Figure 7a is an example).

3. The slope and intercept of this line were then used to "correct" formula (14), and the process repeated. These iterations continued until the resulting slope was 1.0, and the intercept was 0.0.

4. After using *Michaelson*'s [1987] magnitude station corrections for the regressions of step 3, we calculated the mean deviation between individual station estimates of M_Z and the event magnitudes:

$$\delta_i = << M_Z >_j - M_{Z_{ij}} >_{j=1,k} \tag{15}$$

where k is the total number of events that station i has recorded, and $< M_Z >_j$ is the mean M_Z for the jth event. We then recalculated $M_{Z_{ij}}$ and $< M_Z >_j$ for each of our events and repeated steps 3 and 4 until formula (15) approached a stable value, close to zero, for each of our low-gain stations. The sums of these corrections for a given station were then used as that station's site correction, δ.

The resulting final relation for M_Z is

$$M_{Z_{ij}} = -0.71 + 2.95 \log_{10}(\tau_{ij}) + 0.001\,\Delta_{ij} + \delta_i + \gamma_i\,. \tag{16}$$

The final least squares line of step 3 above fits the derivation data set with a residual standard error of 0.225 magnitude units (see Figure 7a). Table 2 is a HYPO71 [*Lee and Lahr*, 1975] format summary listing of these events with the final M_L and M_Z values listed for each event.

We tested M_Z's ability to predict M_L using τ and A_n data from the 196 test events. A least squares line on a scatter plot of M_Z versus M_L, through the 177 test events occurring

in central California, has a slope of .944 and an intercept of .222 which fits the data with a residual standard error of .225 (crosses in Figure 7b). The 19 test set events occurring outside of central California (solid squares in Figure 7b) fall close to this regression line. (Note that the line shown in Figure 7b is the $ML = MZ$ line—not the fit to the test set data.)

As a final check on our choice of 0.001 for the distance term, we plotted M_Z magnitude residuals, $MZres$, as a function of Δ for all 252 events of the combined derivation and test sets (see Figure 11a). A least squares fit to this data yielded the relation $MZres = -0.0014 + 0.00001\Delta$ whose coefficients are sufficiently close to zero to validate the distance term. We note that our distance term is much closer to *Tsumura*'s [1967] value of 0.0014 for Japan than it is to *Lee et al.*'s [1972] value of 0.0035 for central California. We suspect that this difference is due to the fact that for the larger events studied by us and *Tsumara*, the coda is dominated by longer periods than is the case for the small events that dominate the data set of *Lee et al.* [1972]. In addition the larger events studied here produce useable coda length estimates at greater distances than small events; there is a suggestion of larger residuals at short distances in Figures 11a and 11b, consistent with a more rapid coda length fall-off with distance inside 40 kilometers.

Model II

In the second part of this work we solved for a and $b(\omega)$ in *Aki and Chouet*'s [1975] single backscattering model, $A_c(\omega, t) = st^{-a}\, e^{\frac{-b(\omega)}{\log_{10} e} t}$, and directly substituted these values into a formula of the form:

$$M_Z 2 = k + a * \log_{10}(\tau) + b(\omega) * \tau + \delta + \gamma\,, \tag{17}$$

allowing only the value of k to vary in a subsequent comparison with the M_L values of the derivation set. Because of the weak dependance of coda length on epicentral distance we decided to begin without a distance term.

Because *Aki and Chouet*'s [1975] model assumes that coda duration is not a function of epicentral distance, we decided to leave the distance term out of equation (17).

As explained above, the RTP reports up to 6 average absolute value amplitudes, A_n for each seismogram (Figure 5a is an example of a seismogram with these A_n values drawn

in by hand). We fit an $L1$ norm line through these A_n values in $\log A_c(\omega,t) - \log(t)$ space (see Figure 5b). The slope, β, of this line is thus an estimate of the first derivative of the coda decay with respect to $\log_{10}(t)$, at a single station for a single event, at a specific point in time:

$$\beta \equiv \frac{\partial[\log_{10} A_c(\omega,t)]}{\partial[\log_{10}(t)]} . \tag{18}$$

We then plotted β as a function of time, T_k, where T_k is the time at the center of the group of windows whose A_n values were fit using the $L1$ norm. (Column 3 of Table 5 lists these sample times).

Assuming *Model I* for $A_c(\omega,t)$, $\log_{10}\,[A_c(\omega,t)] = \log_{10}\,[\text{source}(\omega)] - a[\log_{10}(t)] + \log_{10}\,[\text{site}(\omega)]$, and

$$\beta = -a . \tag{19}$$

In this case a plot of β as a function of T_k will be a horizontal line (the dotted line in Figure 8b) with y-intercept equal to a, and the slopes of the coda decay in $\log[A_c(\omega,t)] - \log(t)$ space are constant with respect to time.

If, however, one assumes *Model II* for $A_c(\omega,t)$, then $\log_{10}[A_c(\omega,t)] = \log_{10}[\text{source}(\omega)] - a[\log_{10}(t)] - b(\omega)t - \log_{10}[\text{site}(\omega)]$ [*Aki and Chouet* 1975], and

$$\beta = -a - \frac{b(\omega)}{(\log_{10} e)} t . \tag{20}$$

In this case a plot of β as a function of T_k is a line with slope equal to $\frac{-b(\omega)}{\log_{10} e}$ and y-intercept equal to $-a$ (the solid line in Figure 8b) and the slopes of the coda decay in $\log[A_c(\omega,t)] - \log(t)$ space increase with time into the coda as illustrated by Figure 8a.

A least squares line through our derivation set β versus T_k yields a relationship of the form of (20) with $a = 1.51$ and $b(\omega) = 0.0081$ (see Figure 9a), which fits the data with a residual standard error of 0.643. The standard errors, respectively, for the intercept, a, and slope, $b(\omega)$, of this regression line are 0.068, and 0.0015. (In an attempt to remove the effect of station site from these β measurements before performing this regression, we calculated the mean of the deviations of a given station's observed β from the value predicted from an initial, uncorrected regression of the slopes against T_k. Figures 9a and

9b show fits to these corrected β's as a function of T_c. Only those β's derived from good $L1$ norm fits to at least four consecutive coda amplitudes, spanning the onscale portion of the post S-wave coda decay, were used.)

After substituting the values for a and $b(\omega)$ obtained from the fit to our β versus T_k data directly into equation (17), we calculated the average event M_{Z2} for each event. We then adjusted the value of k in (15) for a best fit: $k_2 = k_1 + \frac{1}{n}\sum_{i=1}^{n}(M_L - M_{Z2})$, deriving a final coda magnitude relationship of the form:

$$M_{Z2_{ij}} = 1.41 + 1.51 * \log_{10}(\tau_{ij}) + 0.0081\ \tau_{ij} + \delta_i\ . \tag{21}$$

We thus derive the values for a and $b(\omega)$ in this coda magnitude relationship directly from a fit to the coda amplitude data. A linear least squares regression line through the average event M_{Z2} versus M_L derivation set data has slope of 0.840 and an intercept of 0.840 which fits the data with a residual standard error of 0.185 (Figure 10a).

A linear regression of M_{Z2} on M_L for the central California portion of the test set (Table 3, crosses in Figure 10b) yields a line with a slope of 0.940 and an intercept of 0.396. The values for M_{Z2} for a number of large earthquakes occurring throughout California (the solid squares in Figure 10b) fall close to this regression line. This implies that the M_{Z2} formulation will work at regional distances.

DISCUSSION

Since $\log_{10}(\tau)$ is nonlinear with respect to M_L, duration magnitude scales parameterized solely as linear functions of $\log_{10}(\tau)$ predict M_L well only over some limited magnitude range. M_Z, parameterized in this way, predicts M_L well for events in the M_L 3.3 to 6.5 range (Tables 3 and 4, Figure 7b.). Ultimately, predicting M_L well over the entire magnitude range of interest will require something other than a linear function of $\log_{10}(\tau)$.

Herrmann [1975] demonstrated that the conventional parameterization for M_D as a linear function of $\log_{10}(\tau)$ follows directly from the power law approximation to the shape of the coda decay envelope, $A_c(\omega, t)$. In this case, $\log_{10} A_c(\omega, t) = k - a * \log_{10}(t)$, and

$$\frac{\partial[\log_{10} A_c(\omega, t)]}{\partial[\log_{10}(t)]} = -a\ , \tag{22}$$

and would expect a constant slope to the coda decay in $\log_{10} A_c(\omega, t) - \log(t)$ space.

Aki and Chouet [1975] presented a body of theory and observation which showed that $A_c(\omega, t)$ did not follow the simple power law decay, but required an additional exponential term, resulting in an expression for $\log_{10} A_c(\omega, t)$ of the form, $\log_{10} A_c(\omega, t) = k - a * \log_{10}(t) - b(\omega) * t$ (eq. (7)), whose derivative with respect to $\log(t)$ is,

$$\frac{\partial[\log_{10} A_c(\omega, t)]}{\partial[\log_{10}(t)]} = -a - \frac{b(\omega)}{(\log_{10} e)} t \,. \tag{23}$$

Thus one would not expect the constant slope to the coda decay in $\log_{10} A_c(\omega, t) - \log(t)$ space implied by the power law approximation to $A(\omega, t)$. Instead, for a positive, non-zero value of $b(\omega)$ one would expect steeper negative slopes with increasing time (Figure 8a, and the solid line in Figure 8b are examples). An extension of the logic of *Herrmann* [1975] implies that a simple linear relation between $\log_{10}(\tau)$ and M_L would therefore not be expected to hold for all magnitudes. Since the slope of the coda amplitude relation steepens with time, the coefficient of the log coda length term would also be expected to increase as the magnitude range considered increases (Table 1). We suggest that this accounts for the fact that we obtained a larger value for the coefficient a of the log duration term in equation (3) than was obtained by *Lee et al.* [1972].

Because we obtain a nonzero value for $b(\omega)$ in equation (23) from a direct fit to our coda amplitude data, we argue that *Aki and Chouet*'s [1975] single back scattering model better describes coda decays in the central California coast ranges than does the simple power law of *Aki*'s [1969] single scattering model. Applying the logic of *Herrmann* [1975] to *Aki and Chouet*'s [1975] model implies that a more "correct" duration magnitude parameterization is:

$$M_D = k - a * \log_{10}(\tau) - b(\omega) * \tau + \ldots \tag{2}$$

[*Hirshorn, Lindh, and Allen*, 1988, 1989].

CONCLUSIONS

1) $\log(\tau)$ is non-linear with respect to ML.

2) Aki and Chouet's model for $A_c(\omega, t)$ appears to describe the shape of the coda in central California more accurately than the simple power law model does. We base this conclusion on the fits to our coda amplitude data.

3) Our free values of 1.51 for a, and 0.008 for $b(\omega)$ define an approximate shape for the coda decay envelope in central California of the form $\text{Path}(\omega, t) = t^{-1.51}\ e^{\frac{0.008}{\log 10 \cdot e} t}$. Rough approximations of crustal coda Q are possible from these results. Because a and $b(\omega)$ are functions of physical parameters, $a \sim$ (dimension of scattering volume) over 2, $b(\omega) \sim Q_c(\omega)^{-1}$, it should be possible to extend the formalism to other tectonic provinces with different scattering and absorption characteristics.

4) Our value of 1.51 for a is close to the value of 1.5 obtained by *Frankel and Wennerberg* [1987] which corresponds to the r^{-3} geometrical spreading rate that one would expect for body waves traveling outwards from the source as a sphere. A value of 1.5 for a was also found by *Campillo et al.* [1984] for the geometrical spreading value for P_g waves.

5) Both coda magnitude scales of this work predict M_L equally well for regional and local earthquakes occurring in California (Figures 7b and 9b).

6) Our site corrections, assumed to be predominantly a function of near-surface geology in the vicinity of the station, show the same geographic correlation as observed by *Eaton* [1992]. The southernmost NCSN stations, in the Parkfield area, show strong negative values because of their proximity to younger, unconsolidated material, while stations located on or near bedrock yield positive corrections.

Acknowledgements. We only have coda length estimates from the RTP because of Rex Allen's brilliant analysis and coding, and because of Jim Ellis and Sam Rodriguez's untiring commitment to coaxing 99.99% reliable operation from an incredible collection of antique hardware. Their unflappable good humor under fire has not only made this work possible, but a pleasure as well. Caryl Michaelson provided station corrections, Bill Ellsworth and Jerry Eaton provided insight on a number of magnitude related issues, and Bruce Julian

and Barbara Bekins' guidance made it possible for us to survive our encounters with UNIX. Jerry Eaton and Dave Oppenheimer provided very usefull reviews.

REFERENCES

Allen R. V., Automatic earthquake recognition and timing from single traces, *Bull. Seism. Soc. Am., 68*, 1521–1532, 1978.

Allen, R. V., Automatic phase pickers: their present use and future prospects, *Bull. Seism. Soc. Am., 72*, 225–242, 1982.

Aki, K., Analysis of the seismic coda of local earthquakes as scattered waves, *J. Geophys. Res., 74*, 615–631, 1969.

Aki, K., Physical basis for the duration magnitude and recommended practice for coda magnitude determination, *Proc. of the 17th Assembly of the ESC, Budapest, 15*, pp. 73–77, 1980.

Aki, K., and B. Chouet, Origin of coda waves: Source, attenuation, and scattering effects, *J. Geophys. Res., 80*, 3322–3342, 1975.

Bakun, W. H., Magnitudes and moments of duration, *Bull. Seism. Soc. Am., 74*, 2335-2356, 1984.

Bakun, W. H., J. Bredehoeft, R. O. Burford, W. L. Ellsworth, M. J. S. Johnston, L. Jones, A. G. Lindh, C. Mortensen, E. Roeloffs, S. Schulz, P. Segall, and W. Thatcher, Parkfield earthquake prediction scenarios and response plans, *U.S. Geol. Surv., Open-File Rept. 87-192*, 45 pp., 1987.

Bakun, W. H., and A. G. Lindh, Local magnitudes, seismic moments, and coda durations for earthquakes Near Oroville, California, *Bull. Seism. Soc. Am., 67*, 615–629, 1977.

Bisztricsany, E., A new method for the determination of the magnitude of earthquakes, *Geofiz. Kozlemen., 7*, 69–96, 1958.

Canas, J. A., J. J. Egozcue, and L. Pujadas, Seismic attenuation in sourthern Mexico using the coda q method, *Bull. Seism. Soc. Am., 78*, 1807–1817, 1988.

Campillo, M., M. Bouchon, and B. Massinon, Theoretical study of the exitation, spectral characteristics, and geometrical attenuation of regional seismic phases, *Bull. Seism. Soc. Am., 74*, 79–90, 1984.

Chouet, B. A., Source, scattering and attenuation effects on high frequency seismic waves, *P.H.D Thesis, M.I.T*, 1976.

Chouet, B. A., K. Aki, and M. Tsujiura, Regional Variation of the scaling law of earthquake source spectra, *Bull. Seism. Soc. Am., 68,* 49–79, 1978.

Crosson, R. S., Small earthquakes, structure, and tectonics of the Puget Sound region, *Bull. Seism. Soc. Am., 62,* 1133–1171, 1972.

Darragh, R. B., M. R. McKenzie, and R. A. Uhrhammer. *Bull. of the Seismographic Stations of the Univ. of Calif., 99,* 88pp., 1986.

Eaton, J. P., Harmonic magnification of the complete telemetered seismic system, from seismometer to film viewer screen, *U.S. Geol. Surv., Open-File Rept. 75-99,* 50 pp., 1975.

Eaton, J. P., Frequency response of the U.S.G.S. short period telemetered seismic system and its suitability for network studies of local earthquakes, *U.S. Geol. Surv., Open-File Rept. 77-844,* 40 pp. 1977.

Eaton, J. P., Determination of amplitude and duration magnitudes and site residuals from short period seismographs in northern California, *Bull. Seism. Soc. Am.* 45 pp. 1992.

Frankel A., and L. Wennerberg, Energy-flux model of seismic coda: separation of scattering and intrinsic attenuation, *Bull. Seism. Soc. Am., 77,* 1223–1251, 1987.

Herrmann, R. B., The use of duration as a measure of seismic moment and magnitude, *Bull. Seism. Soc. Am., 65,* 899–913, 1975.

Hirshorn, B. F., A. G. Lindh, and R. V. Allen, Real time signal duration magnitudes from low-gain short period seismometers, *U.S. Geol. Surv., Open-File Rept. 87-630* , 16 pp., 1987.

Hirshorn, B. F., A. G. Lindh, and R. V. Allen, Shape of the earthquake coda: implications for coda-magnitude relations, *Seism. Res. Lett., 59,* 38, 1988.

Hirshorn, B. F., A. G. Lindh, and R. V. Allen, The shape of the earthquake coda in central California; a new magnitude scale from the coda envelope *EOS, 70,* 1207, 1989.

Johnson, C., A robust method of magnitude estimation suitable for local digital seismic networks, Calif. Inst. of Tech. *PhD Thesis,* 332 pp., 1979.

Lee, W. H. K., R. E. Bennett, and K. L. Meagher, A method of estimating magnitude of local earthquakes from signal duration, *U.S. Geol. Surv., Open-File Rept. 72-number* , 28 pp., 1972.

Lee, W. H., J. P. Eaton, and E. E. Brabb, The earthquake sequence near Danville, California, *Bull. Seism. Soc. Am., 61,* 1771–1794, 1971.

Lee, W. H., and R. J. Wetmiller, A survey of practice in determining magnitude of near earthquakes: Summary report for networks in North, Central, and south America, *U.S. Geol. Surv., Open-File Rept. 76-677,* 1976.

Lee, W. H. K., and J. C. Lahr, HYPO71 (Revised): A computer program for determining hypocenter, magnitude, and first motion pattern of local earthquakes, *U.S. Geol. Surv., Open-File Rept. 75-311,* 113 pp., 1975.

Lester, F. W., K. L. Meagher, and R. L. Wesson, Catalog of earthquakes along the San Andreas fault system in central California, July-September, 1973, *U.S. Geol. Surv., Open-File Rept. 76-169,* 38 pp., 1976.

Michaelson, C. A., Coda duration magnitudes in central California: an emperical approach, *U.S. Geol. Surv., Open-File Rept., 87-588,*, 100pp., 1987.

Michaelson C. A., and W. H. Bakun, Spatial and temporal trends in coda duration magnitude residuals in central California, *Eos Trans. AGU, 44,*, 1093, 1986.

Rautian T. G., and V. I. Khalturin, The use of the coda for determination of the earthquake source spectrum, *Bull. Seism. Soc. Am., 68,* 923–948, 1978.

Real, C. R., and T. L. Teng , Local Richter magnitude and total signal duration in southern California, *Bull. Seism. Soc. Am., 63,* 1809–1827, 1973.

Richter, C. F., An instrumental earthquake magnitude scale, *Bull. Seism. Soc. Am., 25,* 1–32, 1935.

Stewart, S. W., and M. E. O'Neil, Calculation of the frequency response of the USGS telemetered short-period seismic system, *U.S. Geol. Surv., Open-File Rept. 80-143,* 83 pp., 1980.

Solov'ev, S. L., Seismicity of Sakhalin, *Bull. Earthquake. Res Inst., 43,* 95–102, 1965.

Tsujiura, M., Spectral analysis of the coda waves from local earthquakes, *Bull. Earthquake Res. Inst., Tokyo Univ., 53,* 1–48, 1978.

Tsumura, K., Determination of earthquake magnitude from total duration of oscillation, *Bull. Earthquake Res. Inst., Tokyo Univ., 15,* 7–18, 1967.

Table 1.

$$MD = k + a*\log(\tau) + c*\tau + \ldots$$

k	a	c	Magnitude Range	
0.28	0.71	------	0.0 -- 2.0	Bakun & Lindh, 1977.
0.74	1.26	0.0006	3.0 -- 4.4	Herrmann, 1975.
-0.17	1.52	0.0016	2.5 -- 4.5	Herrmann, 1975.
-1.01	1.89	0.0009	2.0 -- 5.0	Real & Teng, 1973.
-0.87	2.00	0.0035	0.5 -- 4.0	Lee et. al., 1972.
-----	2.14	0.0050	1.8 -- 3.8	Ellsworth, 1990.
-0.89	2.15	0.0025	1.0 -- 5.3	Bakun, 1984.
-0.81	2.22	0.0011	0.5 -- 6.2	Eaton, 1992.
-2.73	2.59	0.007	4.3 -- 5.5	Herrmann, 1975.
-2.46	2.82	------	1.7 -- 4.0	Crossen, 1972.
-2.53	2.85	0.0014	3.0 -- 5.0	Tsumura, 1967.
-0.71	2.95	0.001	3.3 -- 5.7	Hirshorn & Lindh, 1987.
-3.42	3.12	------	2.1 -- 5.7	Bakun & Lindh, 1977.

Table 2.

DERIVATION SET.
60 earthquakes in the central California coast ranges.
3.2 < ML < 5.7

Date	Orig. Time	Latitude	Longitude	Depth	ML	nML	MZ	MZ2	nZ
85 924	721 29.82	37 29.26	121 41.12	9.33	3.50	5	3.53	3.80	3
851026	1430 50.93	36 49.50	121 34.61	10.08	3.40	6	3.31	3.67	8
851124	1921 39.54	36 1.69	120 52.77	8.99	4.50	6	4.60	4.55	12
851128	1513 56.80	36 35.06	121 2.05	9.65	4.60	6	4.84	4.85	8
86 1 6	1952 42.90	37 0.48	121 27.51	8.70	3.70	6	3.21	3.57	7
86 114	3 7 54.64	36 34.91	121 10.39	6.88	3.40	5	3.64	3.89	3
86 114	3 9 36.02	36 35.15	121 10.66	6.87	4.80	4	4.75	4.72	5
86 126	1920 50.91	36 48.24	121 17.28	9.12	5.50	8	5.68	5.75	8
86 126	2346 54.37	36 49.17	121 17.64	7.22	4.00	6	3.91	4.07	10
86 127	1951 33.79	36 48.21	121 15.80	9.38	3.40	6	3.30	3.63	2
86 329	1624 3.61	37 52.90	122 12.21	13.79	4.10	8	4.19	4.26	3
86 331	1155 39.83	37 28.71	121 41.12	8.78	5.70	6	5.88	5.99	5
86 331	13 5 38.00	37 30.27	121 41.20	6.56	3.40	6	3.30	3.63	5
86 415	925 56.50	36 41.49	121 19.10	4.92	3.60	6	3.68	3.92	5
86 428	1733 47.63	37 28.22	121 41.19	8.24	3.50	6	3.34	3.68	6
86 428	2218 40.34	36 48.36	121 16.13	8.75	3.60	6	3.64	3.86	6
86 515	832 1.85	37 27.98	121 41.19	7.64	3.30	4	3.16	3.57	5
86 531	847 6.92	36 38.40	121 14.94	6.52	3.70	6	3.39	3.70	5
86 531	847 55.58	36 38.29	121 14.80	5.54	4.70	8	4.73	4.70	11
86 6 1	649 34.67	36 37.73	121 13.75	5.77	3.50	4	3.80	3.97	6
86 611	15 8 59.29	36 38.17	121 15.00	7.58	3.50	4	3.90	4.04	7
86 7 8	040 22.84	36 4.08	121 49.47	14.50	4.40	5	4.45	4.44	6
86 8 4	341 41.63	37 25.64	121 46.15	9.38	3.40	2	3.56	3.82	4
86 9 3	431 14.48	37 16.83	121 39.04	9.65	4.10	4	4.05	4.16	5
86 923	1927 56.43	36 3.20	121 49.44	12.71	3.70	3	3.66	3.84	5
861011	517 35.59	37 49.43	121 57.77	10.23	4.20	6	3.97	4.07	2
861027	2 6 45.46	37 10.40	121 34.24	6.25	3.60	6	3.70	3.88	6
8611 1	1450 57.17	37 20.21	121 42.14	7.90	3.40	6	3.28	3.63	4
861211	1418 4.97	37 33.58	121 40.14	2.54	4.10	6	4.22	4.28	5
861229	1528 4.65	37 27.14	121 47.67	7.78	4.00	3	4.36	4.36	9
87 119	8 9 4.62	37 9.51	121 33.29	6.71	4.00	5	3.69	3.90	6
87 130	134 44.27	37 44.05	122 8.05	13.58	3.60	8	3.95	4.07	4
87 214	726 50.33	36 10.27	120 20.46	15.09	5.30	10	5.37	5.30	8
87 228	1624 28.02	37 26.88	121 41.03	8.16	3.90	6	4.05	4.14	8
87 410	451 46.04	37 33.94	121 40.68	3.81	3.40	5	3.41	3.74	5
87 421	1547 15.28	37 26.77	121 47.53	7.71	3.20	6	3.47	3.78	4
87 430	1924 21.90	36 49.82	121 17.63	9.10	4.10	6	4.12	4.23	10
87 7 7	1830 24.60	37 15.22	121 38.29	5.66	3.60	6	3.82	4.00	9
87 826	949 45.80	37 9.27	121 8.61	0.39	3.80	6	3.45	3.74	9
871022	347 59.54	37 47.86	121 44.07	12.58	4.40	8	4.78	4.77	11
871028	1952 29.17	36 36.17	121 12.51	7.90	3.30	4	3.40	3.75	4
8711 7	15 6 0.88	36 35.65	121 11.99	9.04	4.00	6	4.12	4.21	12
8712 2	1114 56.10	37 1.41	121 28.44	6.95	3.70	6	3.41	3.75	6
88 1 2	315 21.28	37 6.81	121 31.44	7.92	3.50	6	3.35	3.71	5
88 1 6	2249 48.17	36 46.71	120 52.79	2.84	4.50	6	4.39	4.41	11
88 2 8	14 9 14.97	37 19.41	121 41.49	7.57	3.90	6	3.78	3.99	7
88 220	839 57.24	36 47.58	121 18.88	9.92	5.10	10	5.10	5.07	12
88 222	743 13.25	35 31.71	119 41.20	16.01	4.30	6	4.62	4.54	5
88 4 4	2041 59.58	36 17.64	120 24.91	10.87	3.60	6	3.73	3.88	8
88 4 4	2045 47.52	36 17.29	120 24.85	10.37	3.70	6	3.45	3.69	2
88 613	145 36.50	37 23.65	121 44.42	10.35	5.30	5	5.45	5.46	13
88 620	1526 38.49	37 7.27	121 31.68	8.09	4.10	8	3.77	3.96	9
88 626	754 25.03	37 28.41	121 47.32	8.33	3.20	4	3.53	3.82	4
88 627	1843 22.28	37 7.49	121 53.78	13.60	5.30	4	5.14	5.12	9
88 726	326 55.64	36 34.58	121 8.69	3.77	4.70	10	4.62	4.63	11
88 824	16 1 45.75	36 33.97	121 8.96	2.38	3.20	4	3.67	3.87	7
881012	1247 30.54	37 21.81	121 43.79	6.41	3.40	4	3.52	3.83	6
881110	5 8 2.82	37 22.55	121 43.69	9.83	4.80	6	4.91	4.88	12
881230	2354 23.99	37 17.19	121 39.66	7.73	4.30	6	4.41	4.45	10
89 4 3	1746 34.22	37 25.94	121 46.21	11.68	4.50	7	5.10	5.05	14

Table 3.

TEST SET; portion in central California.
177 earthquakes in the central California coast ranges.
2.8 < ML < 7.1

Date	Orig. Time	Latitude	Longitude	Depth	ML	nML	MZ	nZ	MZ2
84 123	540 19.80	36 21.60	121 53.87	7.42	5.10	8	5.38	6	5.37
84 123	548 57.41	36 21.30	121 53.05	4.21	3.60	6	3.70	7	3.90
84 123	659 50.86	36 21.74	121 53.62	8.21	4.50	6	4.28	5	4.35
84 123	1958 20.95	36 21.55	121 53.10	4.31	3.60	4	3.25	4	3.60
84 124	1 0 38.86	36 21.37	121 53.31	4.44	3.70	6	3.78	6	3.95
84 126	6 7 16.22	36 7.88	120 11.20	9.20	3.20	6	3.85	4	3.95
84 127	444 34.56	36 16.17	120 24.89	7.53	3.80	6	3.70	7	3.88
84 127	1541 54.46	35 56.77	120 9.42	12.27	2.80	4	3.66	3	3.79
84 210	723 24.89	36 22.81	121 53.49	8.03	4.10	4	4.00	6	4.12
84 219	943 9.33	36 17.02	120 19.60	11.71	4.10	6	4.29	8	4.32
84 318	527 29.44	37 45.84	121 42.78	12.50	4.10	4	4.03	4	4.16
84 326	758 39.68	36 45.29	121 27.94	9.97	4.00	4	4.04	11	4.17
84 327	336 35.33	37 44.48	122 7.20	9.05	4.30	6	4.69	7	4.67
84 424	2115 18.75	37 18.54	121 40.60	9.09	6.20	6	5.96	1	6.18
84 424	2125 21.11	37 15.84	121 38.70	5.72	3.10	4	3.13	4	3.51
84 427	410 24.18	37 7.44	121 31.62	7.74	3.50	5	3.14	3	3.63
84 6 5	1656 20.49	37 15.59	121 35.45	4.38	4.20	6	3.88	6	4.09
84 713	12 8 17.54	37 36.66	121 48.24	6.89	3.30	5	3.14	4	3.56
84 731	2059 15.97	37 22.82	121 43.94	8.96	3.50	5	3.27	3	3.63
84 813	951 35.67	37 16.73	121 38.94	9.44	3.70	4	3.48	5	3.81
84 824	1 5 53.93	37 15.24	121 38.30	5.68	3.60	5	3.74	8	3.96
84 926	2046 5.97	37 20.18	121 42.25	7.82	4.40	4	4.59	7	4.63
841022	4 6 31.28	36 35.70	121 11.96	9.22	3.60	4	3.93	6	4.09
8411 4	1120 19.49	36 33.87	121 9.06	4.13	3.10	4	3.37	6	3.70
85 1 3	1122 26.60	36 11.59	120 18.66	10.96	3.80	6	3.85	5	3.99
85 1 6	1833 25.76	36 36.26	121 12.71	8.75	3.50	4	3.64	5	3.85
85 4 6	1316 18.81	36 35.26	121 6.65	8.13	3.30	6	3.39	6	3.71
85 614	1124 1.72	36 10.44	120 16.53	10.47	3.40	6	3.66	3	3.83
85 627	438 54.87	36 31.82	121 5.44	1.70	3.40	4	3.55	5	3.85
85 8 3	1357 10.57	36 8.17	120 9.50	12.95	3.80	5	3.79	4	3.93
85 8 4	1129 15.00	36 8.35	120 9.38	13.34	4.70	7	4.88	8	4.80
85 8 4	1515 39.32	36 2.75	120 4.14	15.30	4.10	5	4.28	7	4.28
85 8 5	1445 37.63	36 7.13	120 4.72	9.41	4.30	5	4.43	7	4.41
85 9 4	6 0 46.48	37 45.23	122 6.84	11.65	3.10	4	3.18	3	3.57
85 930	945 39.41	36 35.94	121 11.69	7.43	3.20	6	3.26	5	3.63
851028	425 51.98	36 33.48	121 8.83	7.41	3.30	6	3.36	5	3.69
851213	1839 22.18	37 0.56	121 43.02	12.28	3.40	6	3.16	4	3.54
851214	2241 44.07	36 4.77	120 38.04	6.40	3.00	4	3.30	3	3.59
86 127	10 7 36.78	36 48.19	121 16.14	9.12	3.40	6	3.08	4	3.50
86 127	1426 6.13	36 49.34	121 17.32	4.69	3.30	6	3.31	7	3.66
86 219	2349 7.59	36 50.62	121 18.34	8.20	3.10	4	3.15	5	3.54
86 512	23 0 19.47	36 50.53	121 18.31	6.64	3.20	4	3.23	6	3.61
86 6 1	649 3.75	36 37.74	121 13.97	5.64	2.90	4	3.19	4	3.58
86 610	132 58.08	36 38.99	121 16.21	10.10	3.30	4	3.47	5	3.76
86 8 3	9 0 13.99	36 36.05	121 12.02	6.83	3.40	3	3.40	5	3.71
86 820	7 2 16.94	37 7.40	121 32.76	4.61	3.30	3	3.23	3	3.65
86 914	815 55.04	36 52.53	121 20.71	7.15	3.40	4	3.21	4	3.59
861031	1846 14.08	36 57.20	121 33.71	6.21	3.50	6	3.61	9	3.85
861124	15 8 1.11	36 36.95	121 12.97	6.84	3.10	4	3.28	3	3.62
8612 7	1233 8.50	35 21.48	120 57.30	0.96	3.30	4	3.56	3	3.70
861220	219 41.59	37 27.27	121 47.93	7.18	3.60	4	3.84	4	4.01
871222	1436 2.07	36 43.80	120 42.74	0.58	3.80	6	3.80	10	3.95
89 515	1539 37.70	36 42.33	121 19.89	3.98	3.50	4	3.55	5	3.86
89 525	1240 9.49	35 51.85	120 24.48	9.46	3.80	6	4.35	3	4.40

89 622	113	24.14	38	3.90	121	50.82	19.48	4.30	4	4.62	4	4.74
89 7 9	1338	44.43	37	24.66	121	45.36	9.09	3.90	5	3.97	8	4.08
89 718	11 7	21.82	36	54.16	121	21.12	8.56	3.80	6	3.72	12	3.91
89 8 8	813	27.33	37	8.67	121	55.71	14.72	5.40	6	5.29	14	5.24
89 8 8	844	9.63	37	8.48	121	55.59	13.99	4.30	6	4.36	15	4.39
89 8 8	1553	28.01	37	9.48	121	57.12	15.88	4.50	10	4.57	18	4.54
89 930	921	2.38	36	29.99	120	31.16	11.55	4.00	6	3.76	12	3.90
891018	0 4	15.24	37	2.44	121	52.59	16.95	7.00	1	6.85	6	7.63
891018	019	17.20	37	9.62	121	58.84	9.85	4.00	7	3.91	4	4.23
891018	021	4.35	37	4.52	121	51.52	11.94	3.50	5	3.53	4	3.80
891018	023	37.28	37	2.37	121	46.12	4.40	3.90	7	3.84	5	4.01
891018	025	4.57	37	3.01	121	46.89	6.70	4.80	5	4.81	9	4.79
891018	028	45.33	36	57.22	121	42.97	14.11	3.30	5	3.30	4	3.63
891018	029	54.69	37	10.45	121	59.12	7.15	3.20	4	3.31	4	3.65
891018	030	41.33	37	7.43	121	59.09	14.50	4.20	7	4.16	10	4.16
891018	033	36.50	37	8.26	122	0.23	6.88	3.20	3	3.00	3	3.42
891018	035	25.78	37	11.28	122	3.28	10.26	3.90	3	3.65	5	3.87
891018	038	28.02	37	10.03	121	59.30	11.02	4.30	4	4.30	10	4.34
891018	041	23.79	37	11.31	122	3.22	15.00	5.10	4	5.29	12	5.21
891018	045	38.59	36	56.75	121	40.72	11.34	4.00	5	3.92	7	4.01
891018	058	56.19	37	7.32	121	58.77	15.14	3.90	3	3.38	3	3.73
891018	1 1	27.33	36	57.61	121	43.58	14.15	3.10	3	3.51	4	3.77
891018	1 3	59.17	37	6.83	121	50.63	6.67	3.70	5	3.75	5	3.94
891018	1 8	8.97	37	11.91	122	2.68	13.58	3.60	3	3.32	3	3.63
891018	116	19.44	37	10.70	121	59.23	7.39	3.50	5	3.55	5	3.80
891018	121	18.55	36	57.85	121	44.31	14.34	3.90	4	3.80	6	3.96
891018	130	59.51	37	3.88	121	54.47	14.50	3.20	4	3.29	3	3.61
891018	145	57.33	37	1.48	121	47.63	11.54	3.50	5	3.62	3	3.89
891018	2 8	53.80	36	57.50	121	43.46	15.39	3.50	5	3.38	3	3.67
891018	215	44.08	36	49.06	121	32.68	0.63	4.50	7	4.48	5	4.48
891018	226	5.91	37	2.17	121	46.59	4.79	4.20	7	4.09	5	4.20
891018	3 2	43.07	37	6.83	121	52.13	4.50	3.70	6	3.57	4	3.82
891018	321	47.64	37	6.48	121	50.24	4.48	3.90	6	3.87	5	4.03
891018	323	56.18	37	8.18	121	59.35	14.96	4.00	6	4.03	7	4.10
891018	335	45.22	37	6.85	121	51.99	4.51	3.80	6	3.61	5	3.85
891018	346	29.44	37	2.87	121	46.97	13.88	3.70	4	4.39	4	4.45
891018	414	47.95	37	7.95	121	58.97	15.31	3.50	7	3.43	5	3.73
891018	416	32.43	37	3.85	121	53.39	13.88	4.10	7	4.00	8	4.05
891018	425	46.64	37	2.50	121	47.11	8.23	3.70	6	3.45	4	3.73
891018	426	36.60	36	59.69	121	45.98	14.33	3.20	4	3.20	5	3.58
891018	428	14.65	36	58.66	121	45.93	16.04	3.50	4	3.44	5	3.74
891018	450	26.84	37	10.18	122	0.54	10.38	4.30	8	4.31	10	4.34
891018	518	34.08	37	1.75	121	50.70	17.87	4.20	8	4.37	3	4.42
891018	644	56.28	37	10.51	121	59.14	7.32	3.60	8	3.29	3	3.65
891018	1022	4.56	37	1.80	121	47.64	11.93	4.40	8	4.46	10	4.42
891018	18 1	3.49	36	55.91	121	41.82	10.03	3.80	5	3.86	9	3.97
891018	18 6	58.02	36	55.84	121	41.45	9.43	3.50	5	3.25	6	3.62
891019	355	0.25	36	59.69	121	47.49	16.63	4.00	7	3.78	9	3.97
891019	412	43.39	36	55.67	121	39.94	6.59	3.60	6	3.32	9	3.69
891019	845	49.59	36	58.50	121	50.42	10.65	4.00	8	4.18	11	4.20
891019	953	49.95	36	56.26	121	41.28	11.85	4.50	8	4.56	12	4.52
891019	1014	34.72	36	58.19	121	50.25	12.00	4.60	7	5.03	15	4.95
891019	1019	41.74	36	57.98	121	49.81	10.18	3.10	4	3.06	3	3.44
891019	1059	57.62	36	57.55	121	49.61	11.10	3.60	4	3.75	9	3.88
891019	1115	22.43	36	57.55	121	49.64	11.18	3.60	6	3.55	6	3.81
891019	1225	33.15	36	55.94	121	40.74	9.83	3.80	6	3.98	10	4.05
891019	1715	5.44	36	55.31	121	38.97	4.65	3.90	5	3.81	8	4.01
891019	1726	18.38	36	55.33	121	39.40	4.73	3.70	6	3.55	8	3.83
891020	018	20.35	37	5.63	121	55.12	10.90	4.30	7	4.08	11	4.16
891020	812	53.92	37	11.10	122	3.47	14.75	4.00	7	3.71	9	3.92
891021	049	43.06	37	3.17	121	51.41	13.95	4.50	7	4.35	16	4.35
891021	2214	56.45	37	4.18	121	53.69	14.89	4.70	7	4.72	16	4.69

891022	944	57.79	36	55.78	121	40.03	4.89	3.50	6	3.26	7	3.64
891022	1424	36.87	37	0.02	121	48.40	17.28	4.00	7	3.92	12	4.04
891025	127	26.13	37	4.91	121	49.22	11.04	4.70	7	4.56	16	4.56
891025	13 0	41.78	36	53.96	121	38.22	6.24	4.00	4	3.76	10	3.97
891025	22 1	49.27	37	0.15	121	48.21	17.03	4.00	7	3.89	13	4.02
891026	9 1	28.86	37	3.35	121	52.60	12.69	3.70	5	3.69	9	3.90
891030	1117	13.32	37	4.16	121	48.50	10.38	4.00	8	3.60	8	3.87
891031	834	51.13	37	4.16	121	48.20	10.08	3.50	5	3.30	5	3.66
8911 1	8 3	17.25	37	6.56	121	50.02	4.34	3.60	6	3.67	8	3.92
8911 2	550	10.62	37	3.92	121	48.24	10.22	4.70	7	4.57	16	4.53
8911 4	716	4.48	37	46.89	122	9.29	11.51	3.60	8	3.49	6	3.67
8911 5	130	41.83	37	4.40	121	54.67	14.20	4.00	5	3.91	16	4.00
8911 5	1337	33.81	37	3.77	121	53.39	13.83	4.20	6	4.03	19	4.12
8911 7	2342	37.28	37	13.82	122	1.51	10.25	4.20	7	4.10	18	4.20
891114	2116	42.54	37	5.59	121	49.96	5.69	3.20	4	3.29	5	3.69
891130	950	40.22	36	43.40	121	21.76	4.28	3.50	4	3.70	12	3.87
8912 1	1116	50.03	36	41.56	121	19.35	6.34	3.50	4	3.67	13	3.83
8912 1	1237	43.17	36	41.58	121	19.33	6.73	4.40	8	4.24	23	4.27
8912 2	20 2	0.38	37	13.79	122	1.72	10.27	3.90	4	3.40	13	3.76
891218	17 7	30.57	36	42.11	121	20.05	6.32	3.80	5	4.04	16	4.10
891223	1637	44.85	36	27.37	120	26.58	10.14	4.20	6	3.78	17	3.91
90 112	910	22.41	36	25.10	120	47.66	14.42	4.30	6	4.24	17	4.26
90 112	1950	56.18	36	16.91	120	24.31	9.20	3.00	4	3.33	9	3.62
90 125	14 4	31.54	36	41.49	121	19.20	5.81	3.90	5	3.80	12	3.93
90 2 7	1412	14.75	36	57.20	121	41.04	7.19	4.10	7	4.08	18	4.14
90 2 8	947	32.02	36	41.51	121	19.16	5.48	3.30	4	3.50	12	3.72
90 212	148	17.34	36	51.76	121	36.31	8.61	3.80	6	3.46	13	3.70
90 323	1350	18.67	36	51.87	121	36.81	9.86	3.70	6	3.32	11	3.64
90 328	6 8	25.19	36	51.31	121	33.96	6.57	3.60	6	3.46	6	3.79
90 4 6	2055	52.83	37	52.28	121	59.68	9.07	3.70	6	3.93	3	4.14
90 4 6	2241	26.39	37	52.29	121	59.91	10.19	3.90	8	3.93	8	4.03
90 4 7	239	17.48	37	52.77	121	58.60	9.87	4.40	8	4.70	14	4.68
90 4 7	251	11.79	37	52.81	121	58.55	9.24	3.60	5	3.59	3	3.79
90 4 7	20 8	59.29	36	54.05	121	38.17	6.06	4.00	6	3.66	13	3.92
90 410	328	21.40	36	52.62	121	36.90	7.27	3.60	6	3.32	9	3.64
90 418	1338	10.14	36	55.02	121	38.92	8.42	4.40	6	4.74	5	4.64
90 418	1341	38.57	36	55.59	121	39.58	6.13	4.90	8	4.67	19	4.69
90 418	1353	51.23	36	55.71	121	39.60	5.93	5.50	8	5.57	23	5.56
90 418	1452	23.54	36	54.65	121	39.63	10.45	4.00	4	4.21	18	4.27
90 418	1528	16.24	36	56.01	121	40.84	10.92	4.40	8	4.21	15	4.29
90 418	1536	51.24	36	56.52	121	41.05	9.62	4.00	6	3.76	14	3.95
90 418	1546	3.39	36	57.20	121	41.16	7.21	5.10	10	5.28	27	5.25
90 418	16 6	28.22	36	56.18	121	40.67	8.56	3.70	6	3.35	12	3.70
90 418	1619	12.96	36	56.00	121	40.59	8.95	3.90	6	3.75	17	3.97
90 422	2 0	15.34	36	53.96	121	38.14	6.03	3.80	6	3.56	11	3.88
90 428	441	47.21	37	52.95	121	58.19	8.05	4.50	8	4.76	9	4.74
90 428	447	41.14	37	52.42	121	59.16	8.81	4.20	10	4.57	9	4.56
90 428	545	3.80	37	51.63	122	1.02	9.44	3.40	6	3.59	4	3.75
90 516	1718	13.88	36	16.03	120	19.68	9.76	3.20	3	3.36	7	3.69
90 517	1849	48.67	37	22.47	121	43.65	9.59	3.60	7	3.49	9	3.81
90 519	1755	57.99	36	17.40	120	21.84	14.44	3.70	4	3.57	9	3.85
90 7 1	036	41.36	37	24.95	121	45.78	8.31	4.20	4	4.04	11	4.24
90 8 5	652	13.32	36	52.60	121	37.77	10.19	4.00	4	4.23	16	4.31
90 822	2124	5.53	37	12.41	122	3.84	12.47	3.70	4	3.45	7	3.74
90 9 8	1252	2.45	36	40.81	121	18.21	7.14	3.60	4	3.64	8	3.90
90 923	259	52.78	36	48.46	121	32.24	7.47	3.60	6	3.83	5	4.10
91 917	2110	28.77	35	49.16	121	19.98	2.60	5.10	4	5.18	22	5.12
921020	528	8.91	35	55.72	120	28.35	9.98	4.30	4	4.73	18	4.73
921225	335	6.80	35	56.24	120	29.06	10.69	3.20	4	3.47	10	3.84
93 314	713	58.77	35	56.51	120	29.28	11.24	3.00	4	3.57	11	3.91
93 4 4	521	25.28	35	56.44	120	29.52	7.60	4.40	12	4.59	11	4.62

Table 4.

TEST SET; portion outside central California.
19 earthquakes.
5.0 < ML < 7.4

Date	Orig. Time	Latitude	Longitude	Depth	ML	nML	MZ	nZ	MZ2
841123	1912 34.77	37 26.23	118 36.42	12.13	5.50	20	5.69	3	5.52
85 124	1127 21.01	38 9.32	118 48.68	11.02	5.20	8	5.17	5	5.01
85 325	16 5 12.78	37 27.26	118 36.71	7.65	5.10	6	5.24	4	5.13
86 7 8	920 55.40	34 30.51	117 30.10	5.04	6.60	7	6.29	6	6.16
86 713	1347 8.54	33 1.81	118 3.39	5.04	5.80	5	5.64	3	5.42
86 720	1429 45.41	37 34.02	118 26.08	6.70	5.90	7	5.81	3	5.68
86 722	1348 59.51	37 31.74	118 29.53	10.32	5.00	5	5.14	3	4.94
86 731	722 39.75	37 28.34	118 21.95	7.48	5.80	7	5.95	3	5.91
8710 1	1442 18.24	34 1.48	118 7.00	6.52	6.10	8	6.34	1	6.44
901024	615 19.44	38 5.50	119 8.04	7.52	5.70	2	5.73	28	5.57
91 628	1443 56.10	34 22.21	118 5.83	10.66	5.70	4	5.63	8	5.41
91 816	2226 9.59	41 53.38	126 18.73	2.50	5.90	4	5.89	1	5.79
91 817	1929 39.51	40 15.58	124 22.23	5.10	6.00	4	5.86	2	5.78
92 423	450 23.50	34 5.42	116 33.32	5.00	6.10	3	6.28	13	6.11
92 425	18 6 2.50	40 19.54	124 28.14	5.00	6.90		6.47	7	6.64
92 426	741 39.45	40 25.42	124 37.52	19.83	6.20		6.32	12	6.25
92 426	1118 25.55	40 22.88	124 36.12	21.27	6.50		6.15	9	5.79
92 628	1157 34.14	34 14.21	116 22.53	8.14	7.40		7.20	9	7.29
92 628	15 5 47.27	34 58.45	118 10.35	5.00	6.50		6.51	25	6.59

Table 5.

Times of the amplitude samples collected by the RTP.

k	tk	Tk
1	1	
2	3	
3	5	3
4	7	4
5	9	5
6	11	6
7	13	8
8	15	10
9	19	13
10	23	16
11	31	21
12	39	26
13	47	31
14	55	37
15	63	43
16	71	51
17	79	59
18	87	67
19	95	75
20	111	87
21	127	99
22	139	109
23	144	115.5

NOTATION:
k -- A counter; the number (or index) of the window.
tk -- The center time of the window.
Tk -- The center time of the GROUP of windows fit in log-log space.

Table 6.

Loma Prieta Mainshock: ML7. .
(τ's from fits to the coda amplitudes in Log(A)- Log(t) space.)

Station		Epicentral Distance (Km.)	Mz
1	CAOZ	47	6.8
2	BSRZ	51	7.3
3	HQRZ	63	7.2
4	PHPZ	162	6.7
5	PPCZ	165	6.9
6	PMMZ	171	6.6
7	PHOZ	179	7.2
8	PHFZ	183	6.8
9	PGHZ	190	6.8
10	PMCZ	197	6.5
		Average:	6.9

Table 7.

Magnitude Site Corrections (σ).

	Z- Station	σ	# Obs.	Std. Dev.
1	AFOZ	0.000	0	99.999
2	BAVZ	0.206	84	0.265
3	BSCZ	-0.095	70	0.237
4	BSGZ	0.171	129	0.257
5	BSRZ	0.008	140	0.210
6	CALZ	0.229	135	0.288
7	CAOZ	0.206	155	0.259
8	CDVZ	0.175	147	0.222
9	GGPZ	-0.051	1	99.999
10	HCOZ	-0.800	40	0.846
11	HPLZ	0.443	78	0.472
12	HQRZ	0.109	128	0.196
13	JALZ	0.000	0	99.999
14	JBLZ	0.000	0	99.999
15	JLPZ	-0.709	3	0.897
16	JNAZ	-0.712	20	0.744
17	JRXZ	0.000	0	99.999
18	JSFZ	-0.345	162	0.378
19	JUMZ	-0.386	20	0.430
20	KSXZ	0.000	0	99.999
21	LRSZ	0.000	0	99.999
22	LSFZ	0.000	0	99.999
23	MHDZ	0.000	0	99.999
24	MPRZ	0.000	0	99.999
25	MTCZ	-0.148	12	0.255
26	PGHZ	0.418	7	0.470
27	PHFZ	0.213	12	0.311
28	PHGZ	0.000	0	99.999
29	PHOZ	-0.406	55	0.460
30	PHPZ	-0.236	60	0.277
31	PJLZ	-0.112	83	0.197
32	PMCZ	-0.387	32	0.428
33	PMGZ	0.180	3	0.248
34	PMMZ	0.090	22	0.266
35	PPBZ	0.141	8	0.292
36	PPCZ	0.000	36	0.228
37	PVCZ	-0.324	61	0.372
38	LJBZ	0.000	0	99.999
39	RAYZ	0.000	0	99.999
40	SILZ	0.000	0	99.999

FIGURE CAPTIONS

Figure 1. Figure 4 from *Lee et. al.* [1972]. Estimated Richter magnitude, $M_D = -0.87 + 2.00Log_{10}(\tau) + 0.0035\Delta$ versus observed M_L. Note the departure of the data from a straight line above about magnitude 3.5 and below about magnitude 1.

Figure 2. Figure 6b. from *Bakun and Lindh* [1977]. $log_{10}(\tau)$ versus M_L for three different seismograph responses (τ_{usgs} is the average τ for USGS stations). Their preferred duration-magnitude relations for τ_{usgs}, τ_{orv}, and τ_{orvlp} are shown as the solid trace, dashed trace, and dotted trace, respectively. Note that a linear relationship between $log(\tau)$ and M_L fits the data well only over (two) limited M_L ranges.

Figure 3. Map of epicenters of the 60 earthquakes (stars) of the derivation set. Essentially all earthquakes above about $M_L 3.2$ occurring in the central California coast ranges between September, 1985 and April, 1989. Solid squares are the 13 lowgain $NCSN$ stations, all at the same gain, in operation at this time.

Figure 4. Figure 4a. is a map of the epicenters of the 177 earthquakes (stars) of the test set that occurred in the central California coast ranges. This data set includes earthquakes in the $M_L 3.3$ to 7.4 occurring in the same region as figure 3. between January, 1984 and April, 1993. Figure 4b. is a map of the epicenters of 19 large earthquakes in the test set (stars) that were not in central California.

Figure 5. Figure 5a. is a local earthquake seismogram with the 6 RTP A_n values (as described in the text) shown in the unclipped portion of the coda decay. ($t = 0$ is at the time of the P arrival.) (See table 5 for the center times, t_k, of the 2 second windows over which these amplitudes are calculated.) Figure 5b. is the same event in $log(A_n) - log(t_p)$ space with an L1 norm line fit to the 6 values of $logA_n$. The intersection of this line with η, the $60mv$. coda amplitude cutoff threshold, defines the τ measurement for larger events– generally above about magnitude 5.5. Vertical axis is at the time of the P arrival plus 1 second.

Figure 6. A clipped record of the $M_L 6.2$ Halls Valley earthquake of April 24, 1984 with *Aki's* [1969] power law coda decay model drawn in by hand through the unclipped portion of the coda decay.

Figure 7. Figure 7a. is a Scatter plot of average event M_Z versus average M_L for the 60 events of the regression data set. The solid line is the regression line; $M_Z = M_L$ by definition, which fits the data with an RMS of 0.22. Figure 7b. is a similar plot with the $M_Z = M_Z$ line shown for comparison. The

177 events in the central California portion are shown as crosses, and the solid squares are the remaining 19 events of the test set falling outside of this region.

Figure 8. Figure 8a. is a plot of $log_{10}A_c(\omega,t)$ versus $log_{10}(t)$. (Figure 4. from *Canas et. al.* [1988].) Each line corresponds to a single local earthquake occurring along the south-west coast of Mexico. Note the increase in the slope of the coda decay with increasing lapse time. All of these events are between M_b4 and 5. Figure 8b. is a schematic plot of the negative of the slopes (β in the text) of the lines in of figure 8a. versus elapsed time, as measured from the the P-arrival time. The dotted line corresponds to the simple power law model of $A_c(\omega,t)$ with $a = 2.95$. The solid corresponds to Aki and Chouet's [1975] single backscattering model for $A_c(\omega,t)$ with $a = 1.5$.

Figure 9. A plot of our β data, corrected for the measurement site's slope bias as described in the text, versus time measured from the time of the p arrival. Figure 9a. is the regression set data and figure 9b is the portion of the test set data occurring in central California— in the same region as regression set data. The intercept of the regression line is a, the coefficient of geometrical spreading in *Aki and Chouet's* [1975] single scattering model:

$$A_c(\omega,t) = source(\omega)site(\omega)t^{-a}e^{\frac{-b(\omega)}{log_{10}e}t}$$

, and the slope of this line is $\frac{\omega}{2Q_c(\omega)}$. Compare these regression lines to the solid line in figure 8b. While the scatter is considerable, there is certainly some (nonzero) slope to the regression lines.

Figure 10. Figure 10a. is a scatter plot of the average event M_{Z2} versus M_L for the 60 events of the regression set. The least squares regression line through the data is shown. The constants a and $b(\omega)$ in this relationship come directly from the fit of the regression line to our coda amplitude data shown in figure 9a. Figure 10b. is a scatter plot of the average avent M_{Z2} against M_L for the 177 events (crosses) of the test set occurring in central California with the resulting regression line. The solid squares are the remaining 19 events of the test set occurring outside of this area.

Figure 11. Magnitude residuals as a function of epicentral distance in kilometers for the the combined regression and test sets. Figure 11a. is the M_Z site residuals, and Figure 11b. is the M_{Z2} site residuals. Note the tendancy of both duration magnitude scales to overestimate magnitude at epicentral distances of less than about 40km. Also note that M_{Z2}, which incorporates no distance term, underestimates magnitude beyond epicentral distances of about 100km. while M_Z, which does have a distance term, does somewhat better in this distance range.

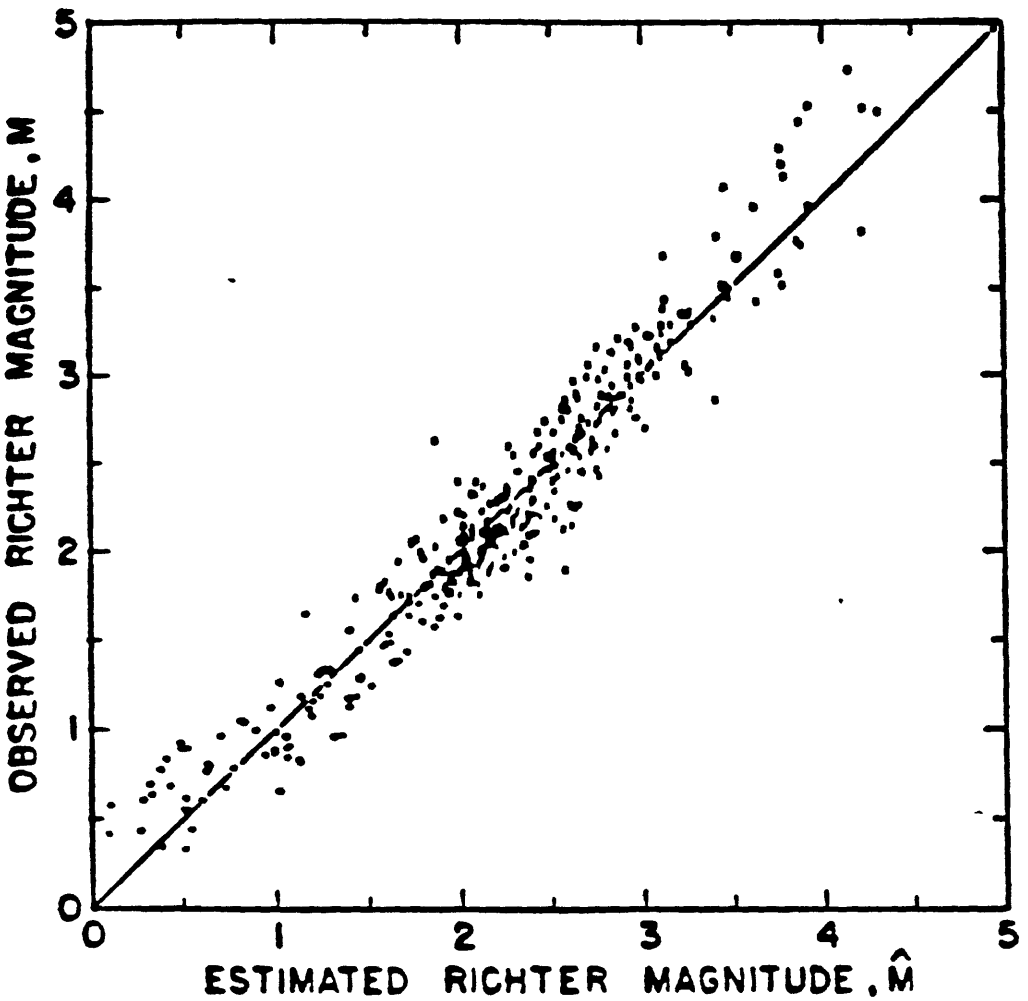
OBSERVED RICHTER MAGNITUDE, M
ESTIMATED RICHTER MAGNITUDE, $\hat{M}$
0
1
2
3
4
5

Figure 1.

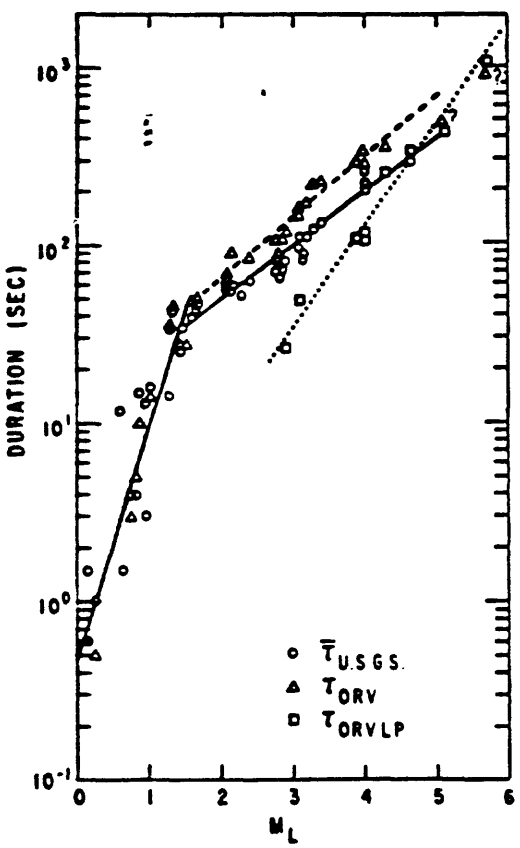
DURATION (SEC)
10^3
10^2
10^1
10^0
10^{-1}
0
1
2
3
4
5
6
M_L
$\bar{\tau}_{U.S.G.S.}$
τ_{ORV}
τ_{ORVLP}

Figure 2.

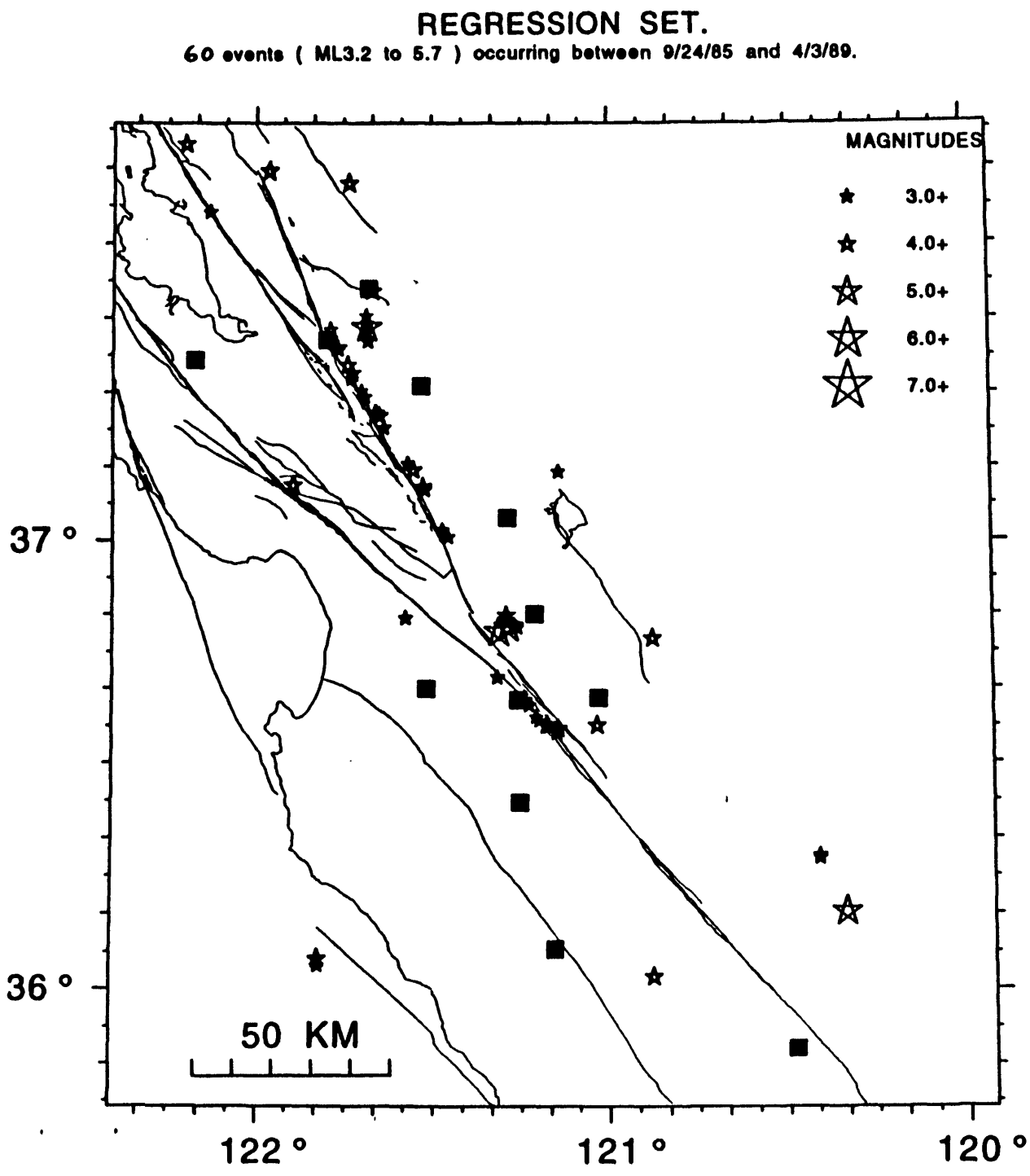
REGRESSION SET.
60 events (ML3.2 to 5.7) occurring between 9/24/85 and 4/3/89.
MAGNITUDES
3.0+
4.0+
5.0+
6.0+
7.0+
37 °
36 °
50 KM
122 °
121 °
120 °

Figure 3.

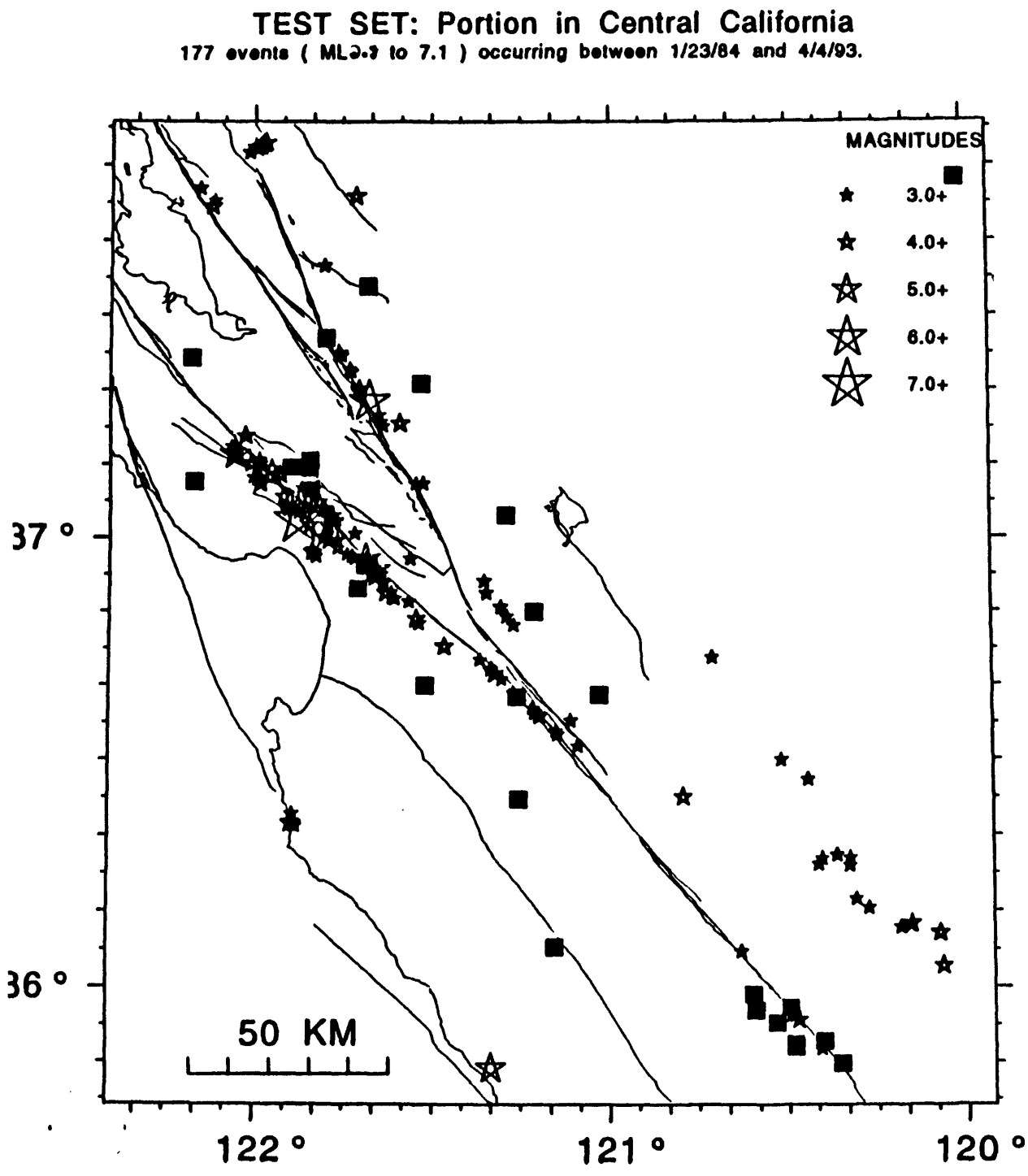
TEST SET: Portion in Central California
177 events (ML3.3 to 7.1) occurring between 1/23/84 and 4/4/93.
MAGNITUDES
3.0+
4.0+
5.0+
6.0+
7.0+
37 °
36 °
50 KM
122 °
121 °
120 °

Figure 4a.

Figure 46.)

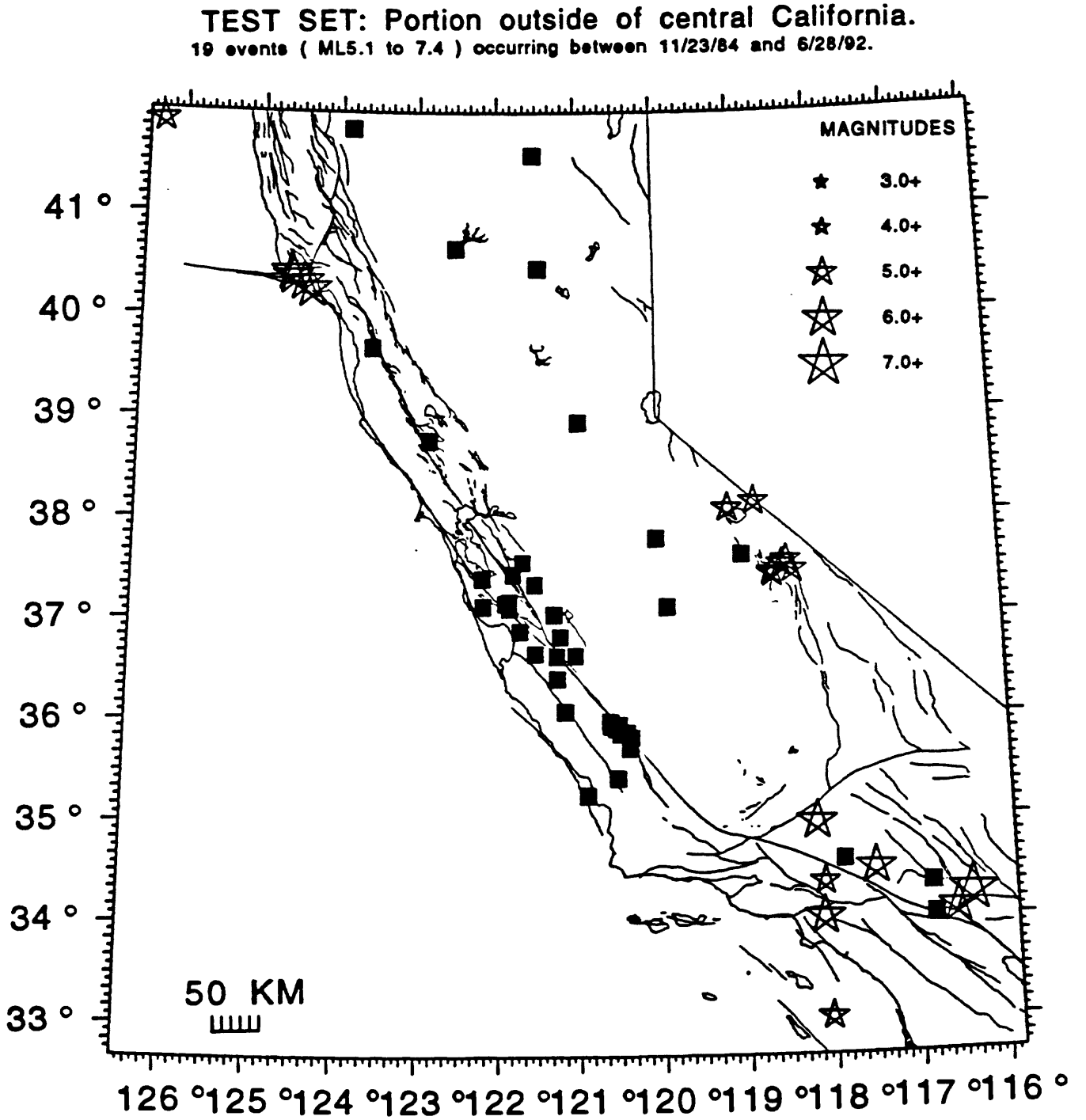
TEST SET: Portion outside of central California.
19 events (ML5.1 to 7.4) occurring between 11/23/84 and 6/28/92.
MAGNITUDES
3.0+
4.0+
5.0+
6.0+
7.0+
41 °
40 °
39 °
38 °
37 °
36 °
35 °
34 °
33 °
50 KM
126 °125 °124 °123 °122 °121 °120 °119 °118 °117 °116 °

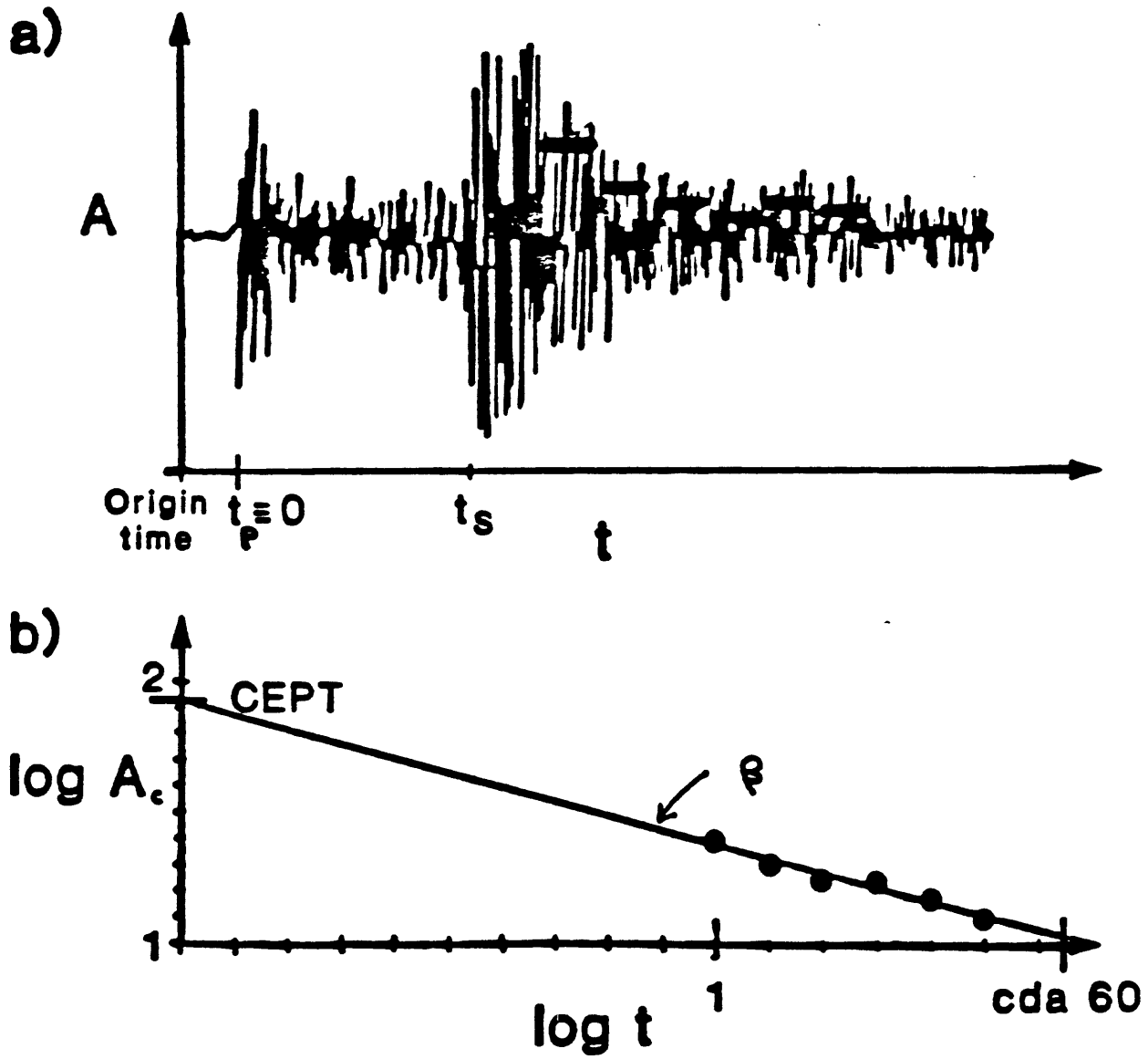

Figure 5.

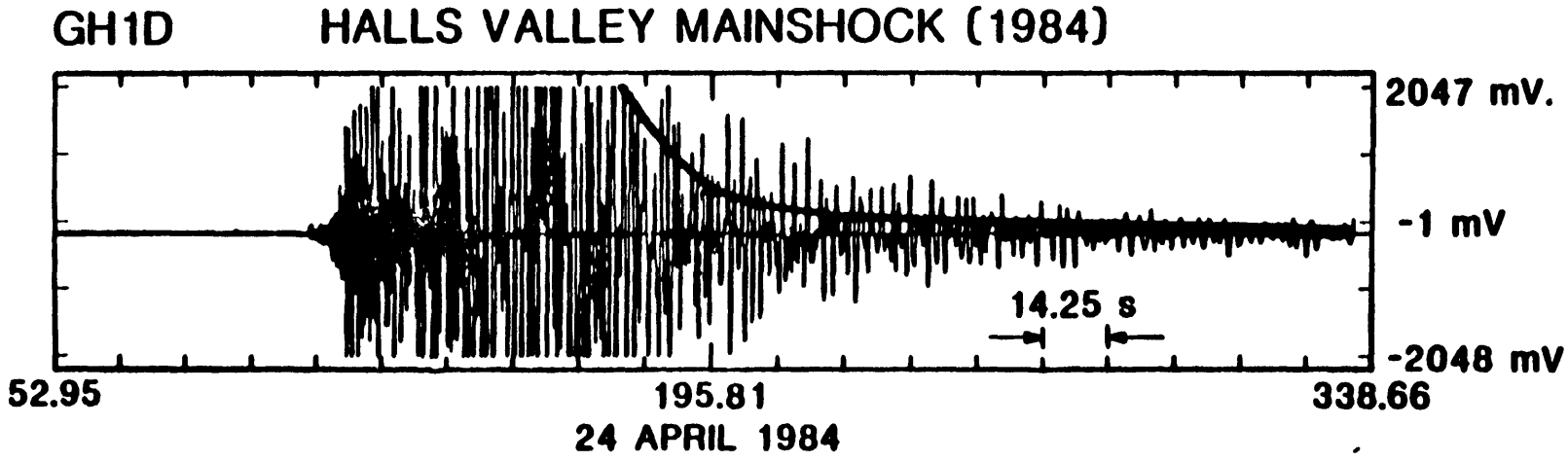
GH1D
HALLS VALLEY MAINSHOCK (1984)
2047 mV.
-1 mV
14.25 s
-2048 mV
52.95
195.81
338.66
24 APRIL 1984

Figure 6

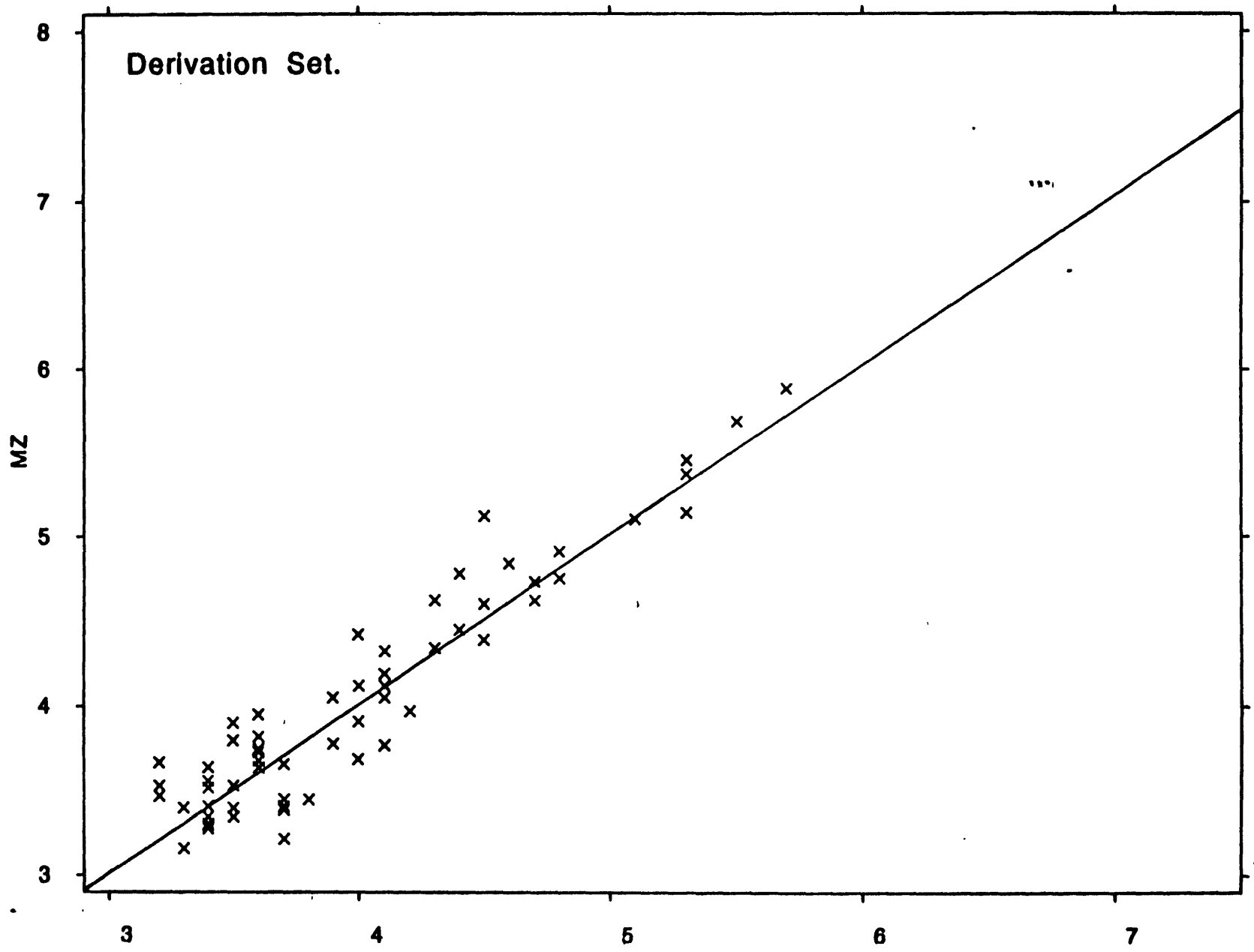

Figure 7a.

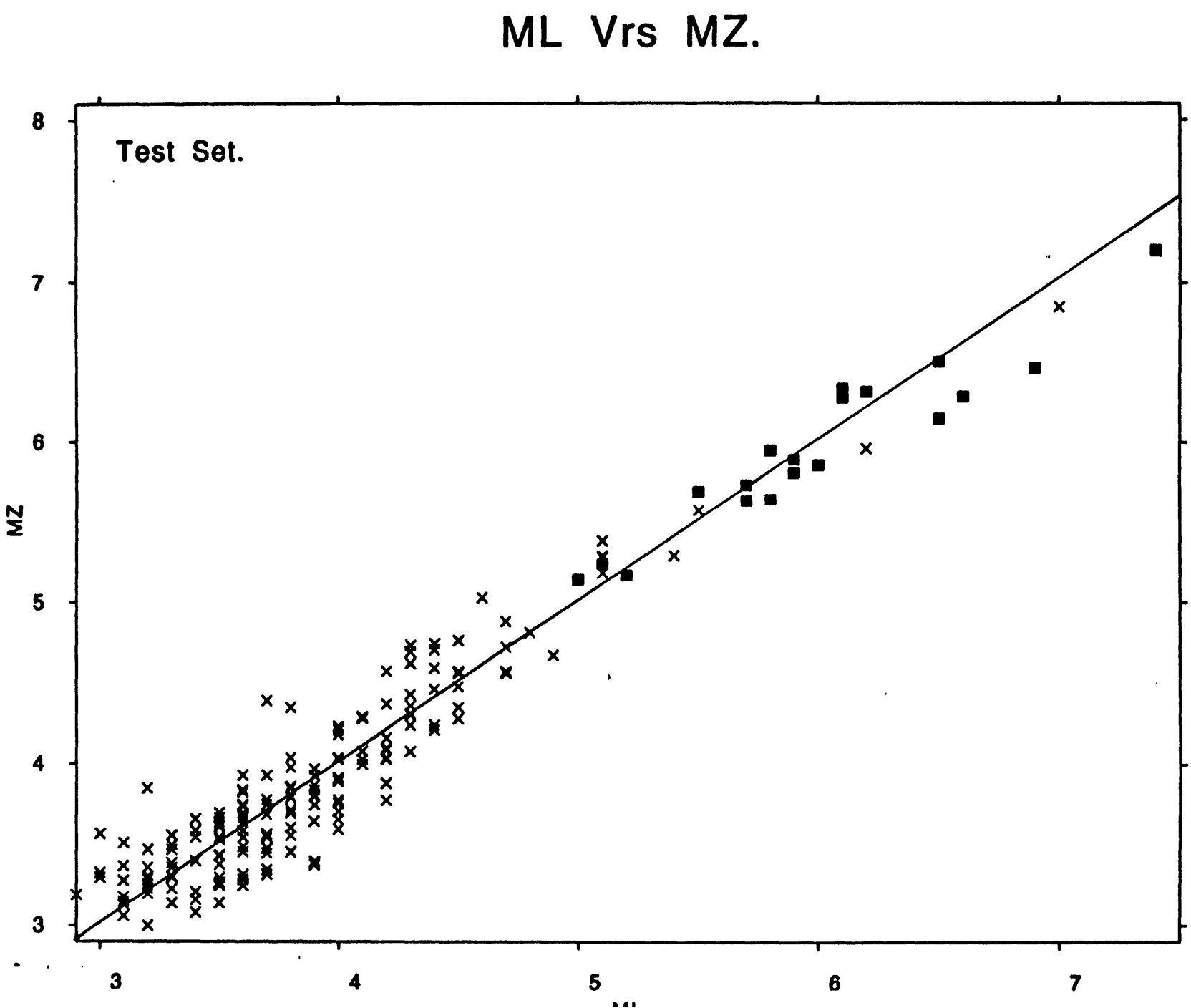

Figure 7b.

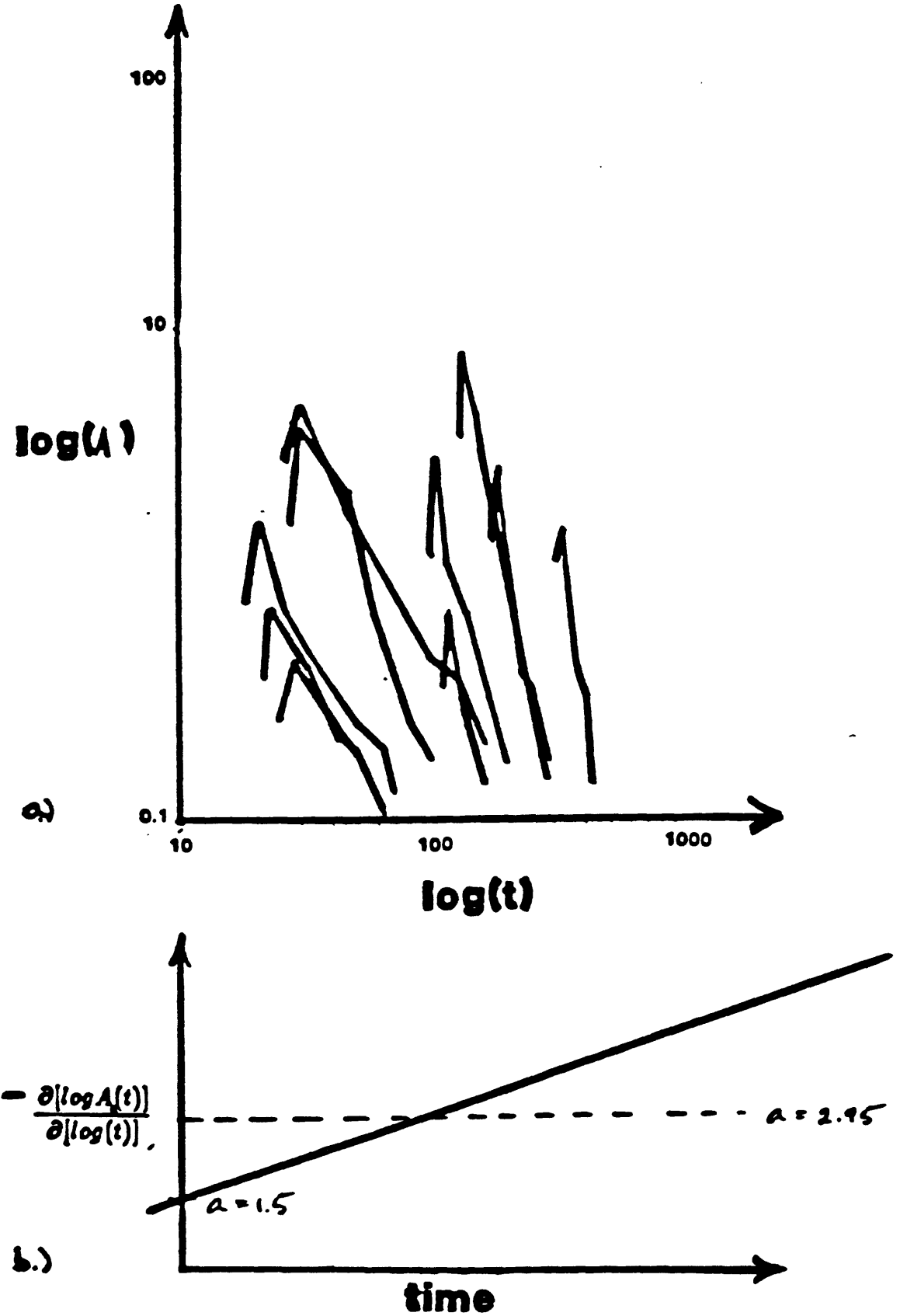
100
10
0.1
log(I)
10
100
1000
log(t)
a)
$-\frac{\partial[\log A(t)]}{\partial[\log(t)]}$
a = 2.95
a = 1.5
b.)
time

Figure 8.

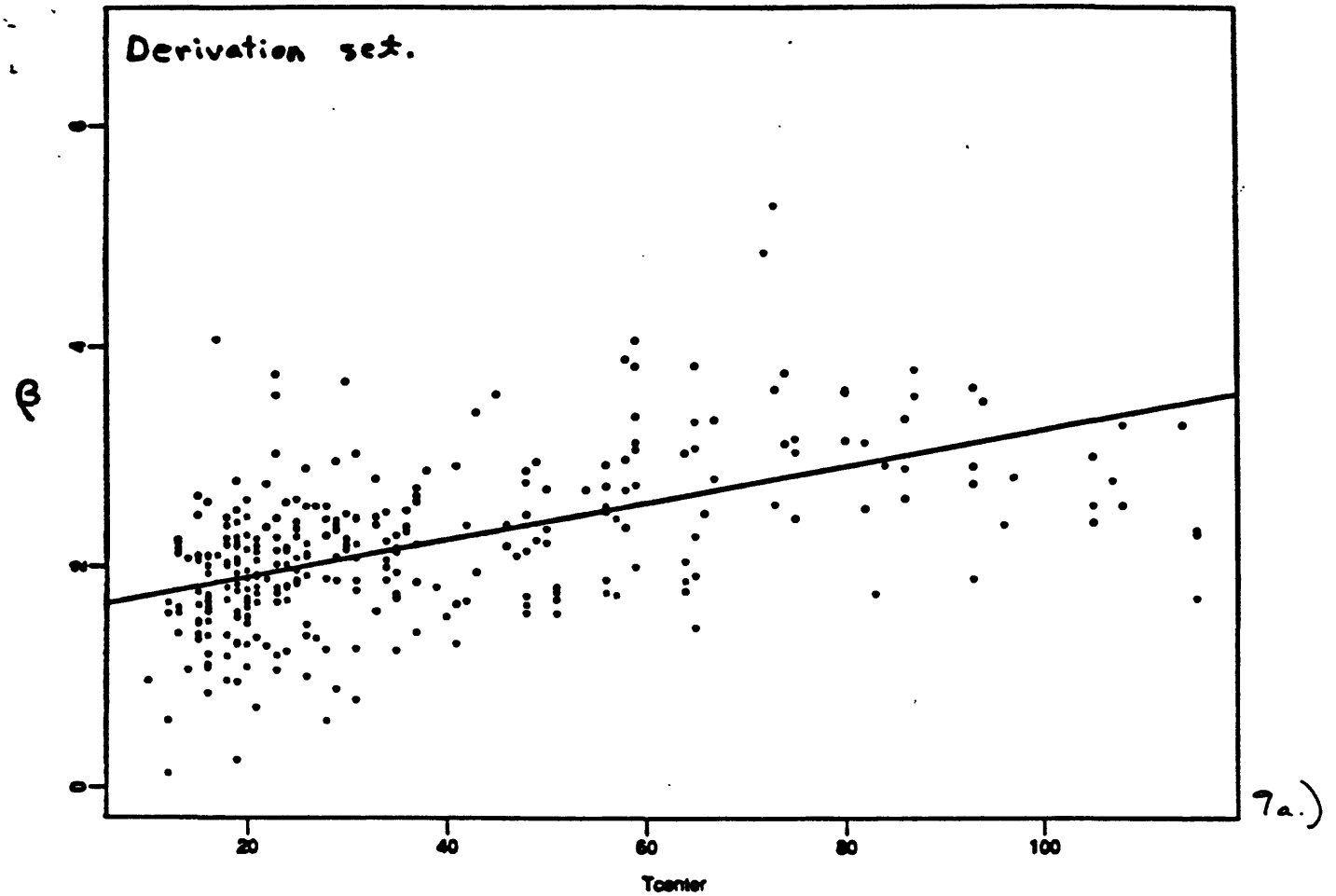

9a.)

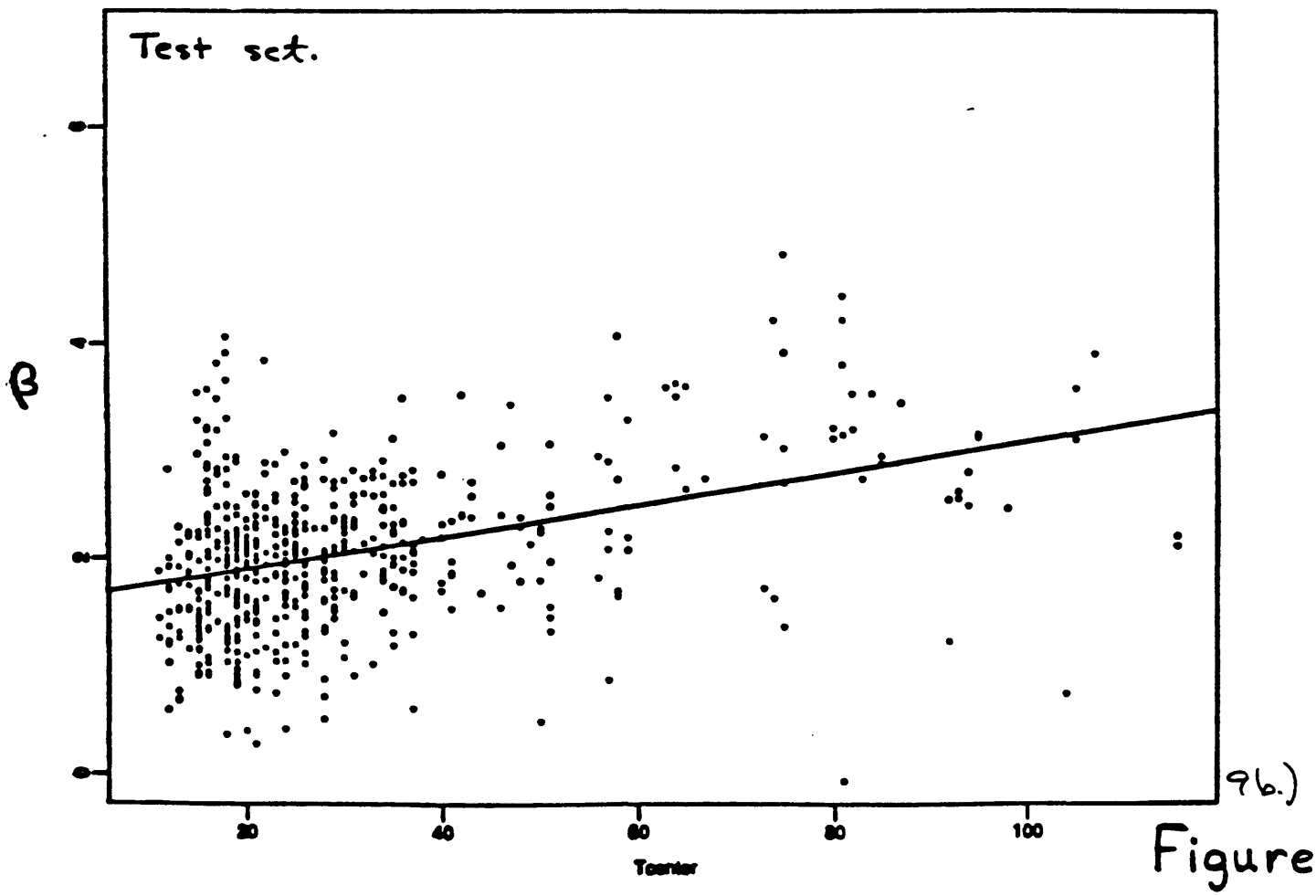

9b.)

Figure 9.

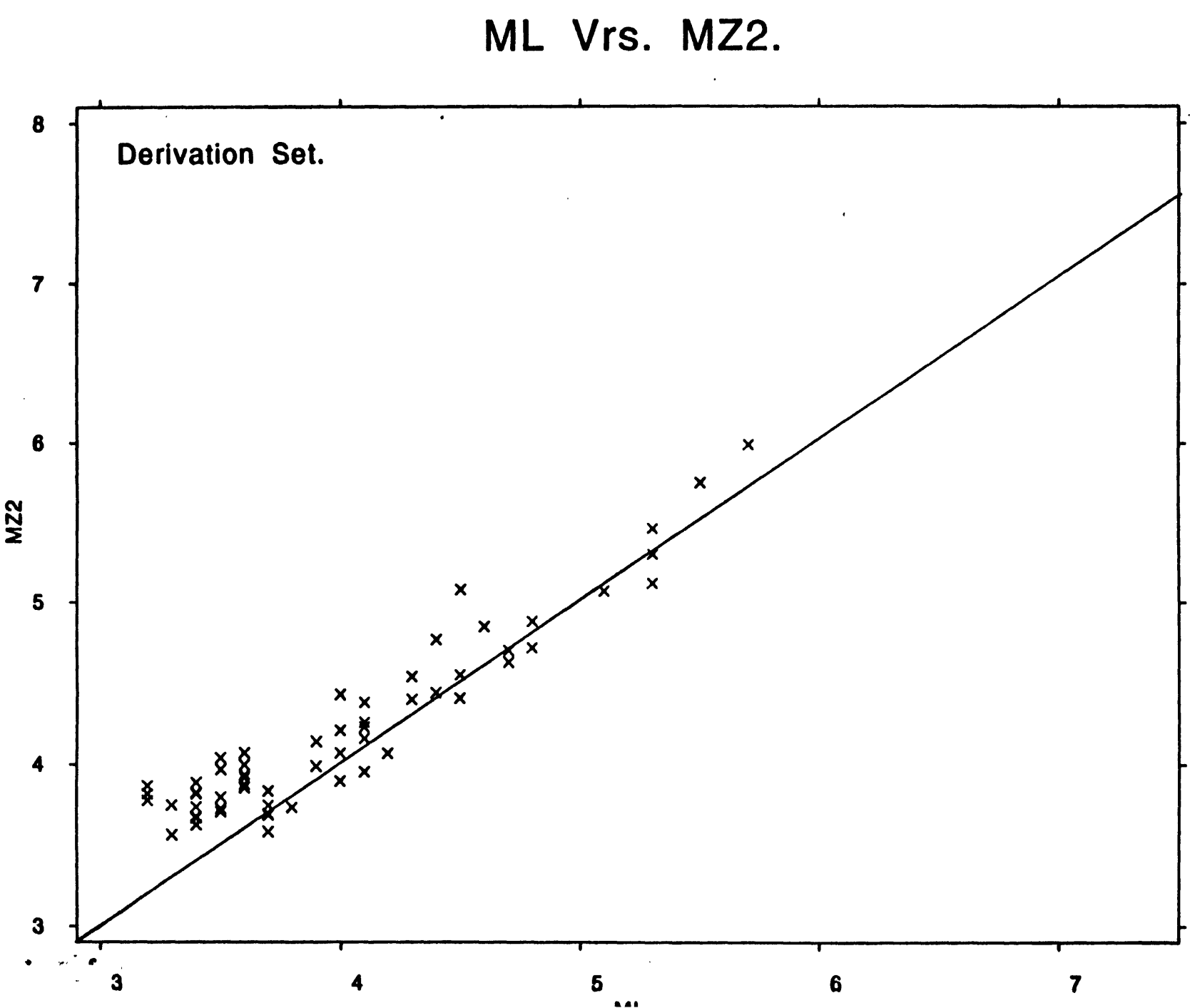

Figure 10a.

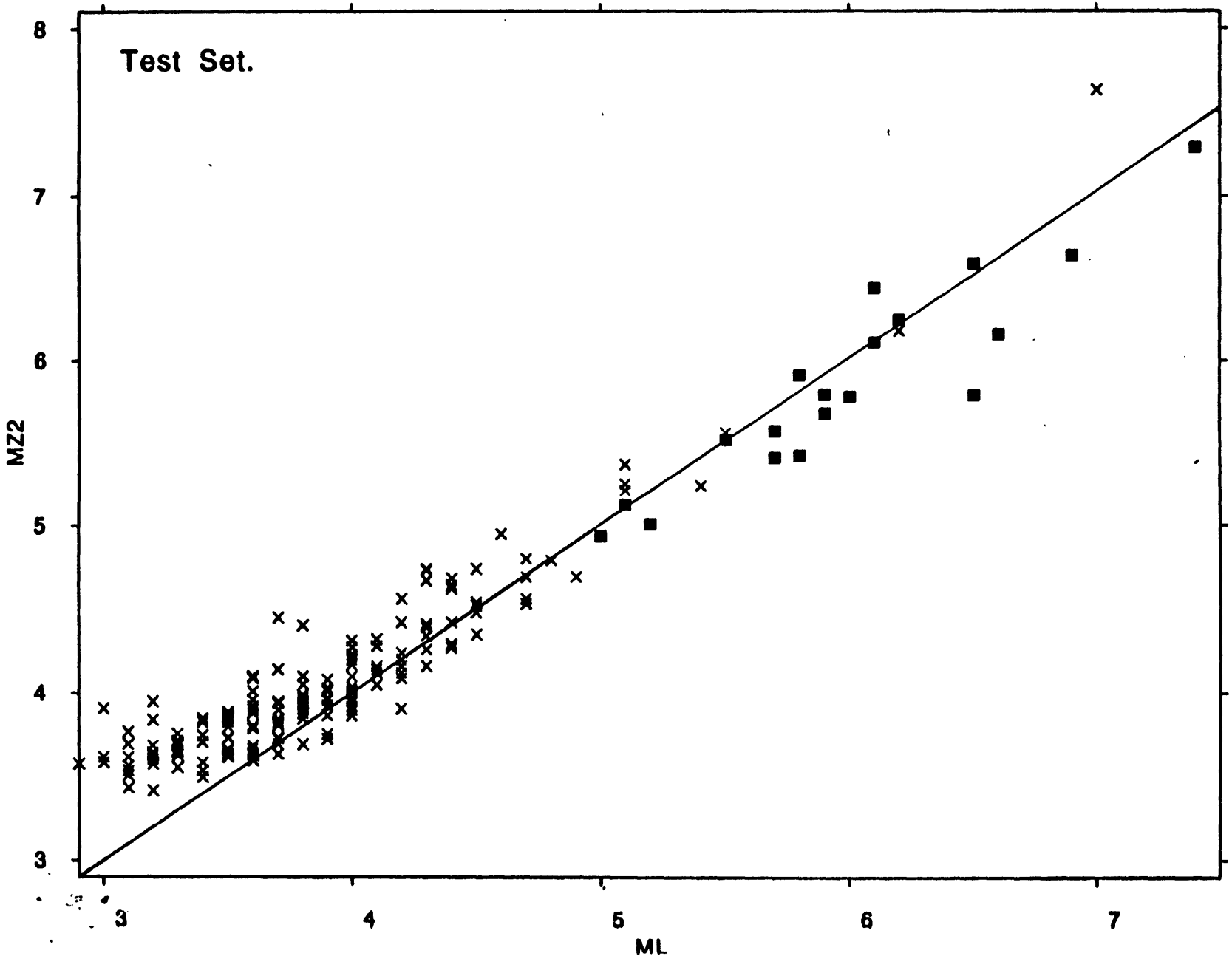

Figure 10b.

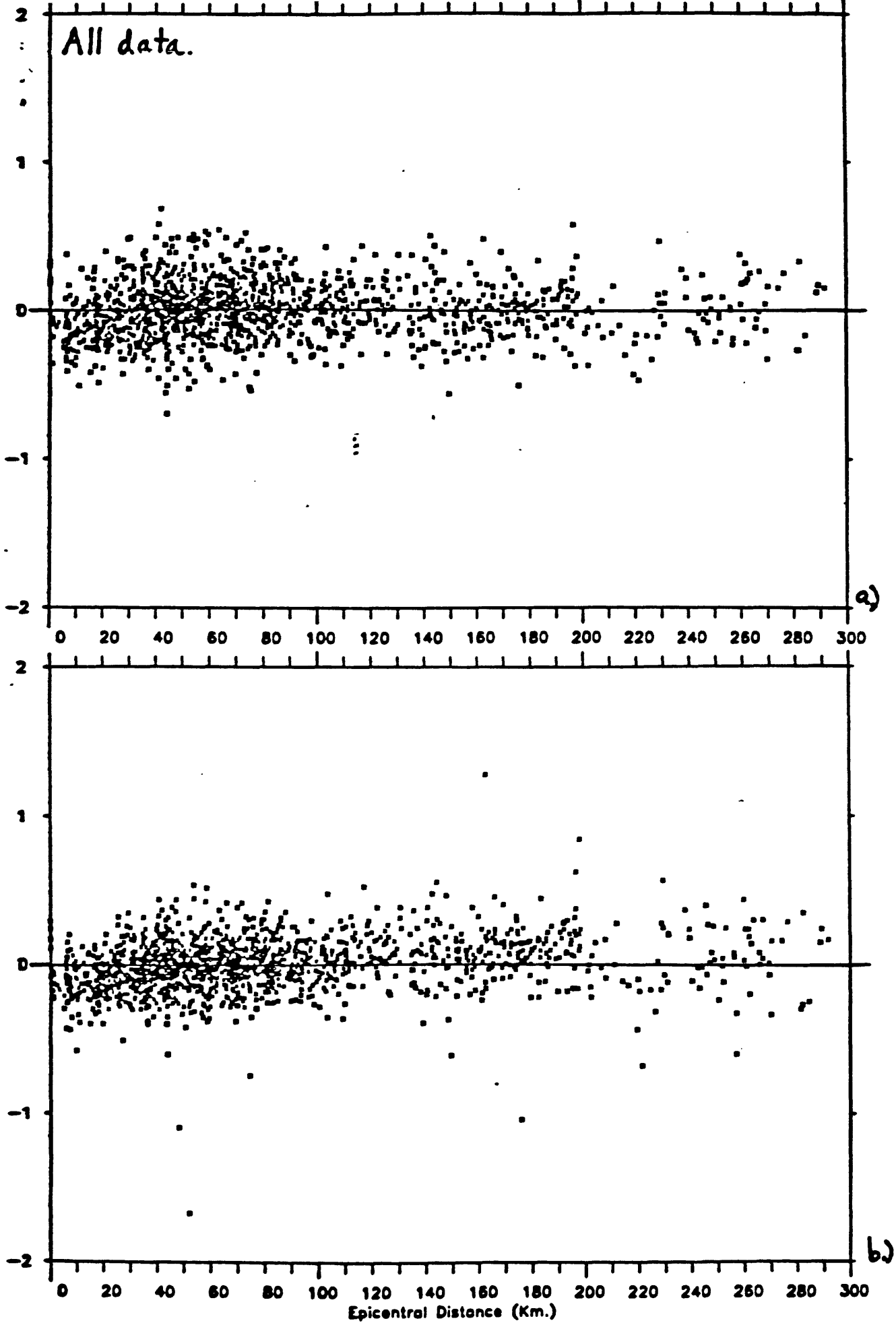
All data.
2
1
0
−1
−2
a)
0 20 40 60 80 100 120 140 160 180 200 220 240 260 280 300
2
1
0
−1
−2
b)
0 20 40 60 80 100 120 140 160 180 200 220 240 260 280 300
Epicentral Distance (Km.)

Figure 11.